

Upper and lower bounds for the mutual information in dynamical networks

M. S. Baptista¹, R. M. Rubinger², E. R. V. Junior², J. C. Sartorelli³, U. Parlitz⁴, and C. Grebogi¹

¹ *Institute for Complex Systems and Mathematical Biology, SUPA, University of Aberdeen, AB24 3UE Aberdeen, United Kingdom*

² *Federal University of Itajuba, Av. BPS 1303, Itajubá, Brazil*

³ *Institute of Physics, University of São Paulo, Rua do Matão, Travessa R, 187, 05508-090, São Paulo, Brazil*

⁴ *Biomedical Physics Group, Max Planck Institute for Dynamics and Self-Organization, Am Fassberg 17, 37077 Göttingen, Germany*

(Dated: October 15, 2019)

We have derived equations to calculate upper and lower bounds for the rate of information exchanged between two nodes (or two groups of nodes) in a dynamical network, the mutual information per unit of time (MIR), without having to calculate probabilities but rather Lyapunov exponents or expansion rates. Since no probabilities need to be calculated, these equations provide a simple way to state whether two nodes are information-correlated and can be conveniently used to understand the relationship between structure and function in dynamical networks. The derivation of these bounds for the MIR employs the some ideas as the ones considered by Ruelle when showing that the sum of the positive Lyapunov exponents of a dynamical system is an upper bound for its Kolmogorov-Sinai entropy. If the equations of motion of the dynamical network are known, upper and lower bounds for the MIR can be analytically or semi-analytically calculated. If the equations of motion are not known, we can employ our equations to measure how much information (per unit of time) is shared between two data sets.

I. INTRODUCTION

Information is an important concept [1]. It measures how much uncertainty one has about an event before it happens and provides a measure of how complex a system is. High-dimensional systems might be actually very predictable, and as a consequence the content of information of such a system can be very limited. But measuring information transfer in complex networks and complex systems is a very difficult task [2, 3]. In the real world, data sets do not always contain a sufficient amount of samples with a sufficient resolution to calculate accurately the probability of events; one needs to develop alternative techniques to measure information as the one proposed in Refs. [4, 5]. As pointed out in Ref. [2], alternative techniques can provide biased results for the value for the amount of information. The reason is that one needs to define the **probability of events** and a suitable **space**. The events need to be relevant in the sense that they contain sufficient information about the process. Besides, defining relevant events, for example the fact that a variable has a value within some particular interval, is a difficult task because the interval is not always known. The calculations of the probabilities are not trivial since they involve space integrals on the probability space.

Measuring the Shannon entropy of a chaotic trajectory is extremely difficult because one has to perform an integral on a fractal set. For chaotic systems that have absolutely continuous conditional measures, one can calculate Shannon's entropy per unit of time, a quantity known as Kolmogorov-Sinai (KS) entropy [6], by summing over all the positive Lyapunov exponents [7] (Lyapunov exponents measure the exponential grow of nearby trajectories). This result is valid for a large class of dy-

namical systems, including the nonuniformly hyperbolic systems [8]. A more general result is due to Ruelle [11], who showed that the sum of all the positive Lyapunov exponents of a dynamical system is an upper bound for the KS entropy. Therefore, the KS entropy (or an upper bound of it), a quantity defined in terms of probabilities of the trajectories in state space, can be calculated by the positive Lyapunov exponents, a quantity usually much easier to be calculated.

Another important concept in the theory of information is the mutual information [1]. It is defined in the following way. Given two systems, X and Y, each one produces events i and j with probabilities $P_X(i)$ and $P_Y(j)$, respectively, the joint probability between these events is represented by $P_{XY}(i, j)$. Then, mutual information is defined as

$$I_S = \sum_i \frac{1}{P_X(i)} \log \left[\frac{1}{P_X(i)} \right] + \sum_j \frac{1}{P_Y(j)} \log \left[\frac{1}{P_Y(j)} \right] - \sum_{i,j} \frac{1}{P_{XY}(i,j)} \log \left[\frac{1}{P_{XY}(i,j)} \right] \quad (1)$$

which is a measure of how much uncertainty one has about an event in X after observing an event in Y (or vice-verse). If the events are continuous one replaces the summation by an integral. In the rest of the manuscript, we simplify the notation for the probabilities and drop the subindexes X , Y , and XY , by making $P_X(i) = P(i)$, $P_Y(j) = P(j)$, and $P_{XY}(i, j) = P(i, j)$.

Obviously, the same difficulties faced to calculate the entropy are present in the calculation of the mutual information. But mutual information is an important quantity to characterize complex systems [3–5, 12], and we should develop alternative methods to overcome such difficulties.

In previous works [13–15], we have proposed an equation to calculate an upper bound for the mutual information rate (MIR), the amount of mutual information per time unit between two equal chaotic systems (the nodes) in a chaotic network. In those, we did not have to calculate probabilities, but only Lyapunov exponents calculated along trajectories on the synchronization manifold, considering that this synchronization manifold can be described by the dynamics of one node. Since these exponents are calculated on a special solution of the considered system, we call these exponents B-conditional Lyapunov exponents (BCLEs). But BCLEs [16] defined in Ref. [15] are different from the conditional Lyapunov exponents (CLEs) defined in Ref. [17] whose definition is explained in Ref. [18]. The main difference is that the BCLEs have physical meaning even when the nodes of a network are complete out of synchrony, as long as the network admits a synchronization manifold. On the other hand, the CLEs have a physical meaning only when the trajectory of the nodes of a network are very close to the synchronization manifold. Therefore, our previous work is only valid for networks whose nodes have equal dynamical description.

The approach in Refs. [13–15] offers us a way to understand how the connecting topology influences the amount of information being transmitted and how the level of chaos at each node forming the network influences the transmission of information. In particular, in Refs. [13, 14] we have shown how to calculate an upper bound for the MIR in networks composed of identical chaotic oscillators with particular connecting topologies. Those works were extended to chaotic networks composed of neurons connected both through electrical (linear) [15] and chemical (non-linear) synapses (connecting functions) [19].

In this work, we propose equations (Sec. II) to calculate upper and lower bounds for the MIR between two nodes in very general chaotic networks or between two scalar signals that have deterministic behavior, meaning that the spreading of nearby points can be described by either the Lyapunov exponents or the expansion rates (Sec. V). This result extends our previous work to more realistic networks whose nodes are not equal. If the network is uniformly hyperbolic and produces a constant invariant measure, our bounds should provide the exact value of the MIR. The derived bounds for the MIR between 2 nodes (or a group of nodes) depend on the Lyapunov exponents or the expansion rates measured on the subspace of the network that is formed by these 2 nodes (or a group of nodes). On this subspace, the number of positive exponents measured coincides with the number of dimensions Ω of the projection (assuming that the number of positive exponents of the network is larger than Ω). If the Lyapunov exponents of the network are known, in Sec. VIII, we have derived upper bounds for the MIR in terms of the Lyapunov exponents of the network that are invariant to the subspace chosen, but depend on the dimensionality of this subspace.

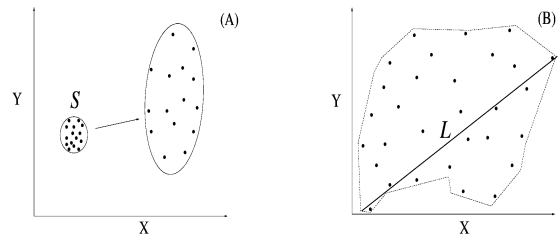


FIG. 1: (A) A collection of points initially within the small ball on a plane are mapped to the large ellipsoid after a time interval τ . (B) After a time interval t , the points initially in the small ball spread all over the attractor within the area delimited by the dashed line. The length L of the thick line represents the largest size of the attractor.

Our theory was applied to understand the exchange of information in systems of two linear and nonlinear coupled maps, large networks of coupled piecewise linear maps, experimental networks of Chua’s circuits, and a reaction-diffusion system of equations that model an excitable media, known as Barkley model [20].

II. UPPER AND LOWER BOUNDS FOR THE MUTUAL INFORMATION RATE

Imagine a network formed by K nodes. We define the subspace Ω where mutual information is being measured to be composed by two nodes \mathcal{X} and \mathcal{Y} , whose state variables are X and Y . We consider that this subspace Ω is 2-dimensional with a domain given by $[\min(X), \max(X)] \times [\min(Y), \max(Y)]$. The set of points (X, Y) belonging to Ω is called the “attractor” and is represented by the symbol Σ .

The subspace Ω is coarse grained in a grid of N^2 boxes with equal sides ϵ , so $N = 1/\epsilon$. The probabilities appearing in Eq. (1) are calculated using this coarse grained space. There will be $i = 1, \dots, N$ columns and $j = 1, \dots, N$ lines. $P(i)$ is the probability of finding points in a column i , $P(j)$ of finding points in the line j , and $P(i, j)$ the probability of finding points in the square box (i, j) appearing where the column i meets the line j .

Our work applies to deterministic systems defined in the following way:

Definition 1 (determinism and the quantity T). (See Fig. 1(A-B)) *Points in the space Ω possess deterministic behavior if expansion rates can be well defined, i.e., given a set of nearby points, for a finite time τ , the evolution of these points spreads out in an exponential fashion all over the attractor Σ [see 1(B)]. Calculating τ over many small regions and taking the average produces the quantity T . For a typical set of nearby points, T should be on average the shortest time interval for these points to spread all over Σ . But for a time $t < T$, this initial set of points evolves to some localized region in Ω , smaller than Σ , but larger than the initial region [see 1(A)].*

To derive our equations and to formally define all the necessary quantities to calculate upper and lower bounds for the MIR, we will consider in our derivation that we have a network formed by a number K of 1-dimensional hyperbolic chaotic systems connected under some topology, and there are K positive Lyapunov exponents. So, the spreading of points under the dynamics is governed by the Lyapunov exponents.

As we will show in the following (Eq. (20)), an upper bound for the MIR is given by

$$I_C = \lambda_1(2 - D) \quad (2)$$

with

$$I_C \geq \frac{I_S}{T}, \quad (3)$$

where λ_1 represents the largest positive Lyapunov exponent measured in the subspace Ω , and

$$D = \frac{\log(N_C(t=T))}{\log(N)}. \quad (4)$$

The quantity $N_C(t)$ is a hypothetical number that represents the number of boxes of sides ϵ that would contain points in the space Ω if points initially in a box of sides ϵ would spread out exponentially fast with a rate given by the the positive Lyapunov exponents on the subspace Ω . After a time t these points should spread out on average by $\exp(\sum_i \lambda_i t)$, where $\exp(\sum_i \lambda_i)$ represents the sum of the positive Lyapunov exponents on the subspace Ω .

The reason why we set $t = T$ is because we want to define an ‘‘universal’’ interval of time to calculate D . This ‘‘universal’’ time T is calculated using Eq. (14).

The quantity I_S in Eq. (3) is defined in Eq. (1) and depends on the probabilities $P(i)$, $P(j)$, and $P(i, j)$. The quantity I_S/T represents the ‘‘exact’’ value of the MIR. Inequality (3) means that the average gain of information per time unit cannot be larger than I_C .

So, D is defined in a similar way as the capacity dimension [21], denoted as D_0 . However, it is not the capacity dimension. Since Ω is considered to be a projection of the whole phase space and D might differ from the capacity dimension measured in the full dimension phase space. Denote \tilde{D}_0 to be the capacity dimension of the set Σ on the subspace Ω . Make $|\tilde{D}_0|$ to represent the non-integer part of D_0 . Typically, $|\tilde{D}_0| \geq |D_0|$, since the projection of Σ on Ω fills out the gaps on a fractal structure. The quantity D here defined typically satisfies

$$D \leq \tilde{D}_0 \quad (5)$$

and, therefore, if we define

$$I_C^l = \lambda_1(2 - \tilde{D}_0), \quad (6)$$

we should have that

$$I_C^l \leq I_C. \quad (7)$$

The explanation for inequality (5) can be seen in Sec. II B.

We will then show (see 3 paragraphs before Eq. (17), Sec. III C, and Sec. IV) that if the points occupy boxes in the space Ω uniformly, i.e., $P(i, j)$, $P(i)$, and $P(j)$ is a constant for all i and j then

$$I_C^l = \frac{I_S}{T}, \quad (8)$$

and if additionally the spreading of points is uniform and $D = D_0$, obviously

$$I_C = I_C^l = \frac{I_S}{T}. \quad (9)$$

Otherwise (see 3 paragraphs before Eq. (17)), if the occupation of boxes is only partially non-uniform [$P(i) = P(j)$ for all i and j , but $P(i, j)$ is not equal for all i and j], or everywhere non-uniform [$P(i) \neq P(j)$, and $P(i, j)$ are not constant], we have that I_C^l represents a lower bound for the MIR and, therefore,

$$I_C^l \leq \frac{I_S}{T}. \quad (10)$$

We will finally show (see Eq. (28)) that Eq. (2) can be written in terms of the two largest Lyapunov exponents measured on the subspace Ω .

Defining \tilde{N}_C to be the number of occupied boxes on the space Ω , when this space is coarse grained by boxes of side ϵ , then the capacity dimension of the set Σ projected on the space Ω is given by

$$\tilde{D}_0 = \lim_{\epsilon \rightarrow 0} - \frac{\log(\tilde{N}_C(\epsilon))}{\log(\epsilon)}. \quad (11)$$

The time $\tau^{(i,j)}$, representing the time that points inside an initial box $C^{(i,j)}$ take to spread out throughout the attractor can be estimated by the time interval, $\tau_{min}^{(i,j)}$, that such points take to firstly return to that same box [22], since for that to happen the iterated points should be spread all over the attractor. So,

$$\tau^{(i,j)} \approx \tau_{min}^{(i,j)}, \quad (12)$$

and T can be calculated from $\tau^{(i,j)}$ by

$$T \approx \frac{1}{\tilde{N}_C} \sum_{i,j} \tau^{(i,j)}. \quad (13)$$

Assuming that the regions S , where τ_{min} is measured, are boxes with equal sides ϵ , and that the size of the attractor Σ is L , T can be estimated by solving the equation $\epsilon\sqrt{2} \exp^{\lambda_1 T} = L$, which takes us to

$$T \approx \frac{1}{\lambda_1} \log \left[\frac{L}{\epsilon\sqrt{2}} \right], \quad (14)$$

where λ_1 is the largest Lyapunov exponent measured on the subspace Ω . A derivation of Eq. (14) can be seen

in Sec. II C. For more information about this equation, see Ref. [23], which is constructed based on the principle that after a time T , points inside a box typically have the shortest first Poincaré return times to it [23, 24].

The reason for T appearing in the denominator of Eq. (3) can be explained as in the following. Mutual information depends on the resolution with which the phase space is partitioned, or on the number of bins considered to define probabilities. The larger the number of bins, the larger can be the mutual information. So, it is an usual practice to normalize the mutual information to a quantity between 0 and 1. The normalization is done by dividing I_S by $\log(N)$, where N is the number of partitions in every data set. $\log(N)$ is the maximal possible mutual information one can have from two discrete sources that are being measured with a resolution of N partitions or bins. Therefore, the quantity T in Eq. (3) can be interpreted as a normalization constant providing, in this case, the production of mutual information per time unit, instead of mutual information per number of bins, as it would be the case if we had used $T = \log(N)$ in Eq. (3).

To illustrate Eq. (2), imagine two completely synchronous chaotic maps. Then, $D = 1$, and $I_C = \lambda_1$. For two completely decoupled chaotic maps, $D = 2$, and therefore, $I_C = 0$.

This aspect of our work is similar to the work of Ref. [25], in the sense that both methods do not directly calculate probabilities when estimating the mutual information. In Ref. [25] mutual information was calculated by estimating probabilities of events from the distance of points in the data set. Our approach instead is aimed at estimating bounds for the MIR. In fact, one advantage of our approach is the simplicity with which bounds for the mutual information can be calculated. The other is that our approach calculates bounds for the mutual information in terms of well known quantities in dynamical systems. Our approach takes advantage of the idea that we can estimate bounds for the MIR if we know how fast nearby points spread out.

A. Upper bound for the MIR

In order to proceed, let us consider Shannon's entropy which is defined as

$$H_S = \sum_i \frac{1}{P_i} \log \left[\frac{1}{P_i} \right]. \quad (15)$$

To derive Eq. (2), let us first understand, using a simple example, the relation between the KS entropy and the sum of the positive Lyapunov exponents. From that, the ensuring derivation of Eq. (2) is straightforward. Consider two coupled systems, possessing two positive Lyapunov exponents, λ_1 and λ_2 , with $\lambda_1 \geq \lambda_2$. Points inside an ϵ size box spreads out according to the Lyapunov exponents (see Fig. 2). If the sides are oriented

along the orthogonal basis used to calculate the Lyapunov exponents, the points spread out after a time interval n to $\epsilon\sqrt{2}\exp^{\lambda_1 n}$ along the direction from which λ_1 is calculated. The points spread after a time interval n to $\epsilon\sqrt{2}\exp^{\lambda_2 n}$ along the direction from which λ_2 is calculated. After an interval of time T , these points spread out all over the attractor Σ . We assume that $N_C = \tilde{N}_C$, for any initial box of points. Thus, the number of boxes of side ϵ that fit inside Σ can be calculated by $N_C = 2\epsilon^2 \exp^{(\lambda_1+\lambda_2)T} / 2\epsilon^2 = \exp^{(\lambda_1+\lambda_2)T}$. The KS entropy is just the Shannon's entropy divided by the time interval considered to produce that entropy.

The KS entropy can be defined as

$$H_{KS} = \lim_{l \rightarrow \infty} \frac{1}{(l-1)} \sum_{i=1}^{l-1} [H_S(n=i) - H_S(n=i-1)], \quad (16)$$

where $H_S(n)$ represents the Shannon's entropy of a set of points after being iterated n times.

At the iteration $n = 0$, there is only one box and the probability of finding points in that box is equal to 1. Shannon's entropy [Eq. (15)] $H_S(n = 0)$ is zero. At the iteration $n = 1$, there are $N_C = \exp^{(\lambda_1+\lambda_2)}$ boxes (see Fig. 2). So, assuming that the spreading of points is uniform, the probability of finding points in one box at the iteration $n=1$ is given by $P = 1/N_C$. Therefore, Shannon's entropy at the iteration $n=1$ would give $H_S(n = 1) = N_C \frac{1}{N_C} \log(\exp^{(\lambda_1+\lambda_2)}) = \lambda_1 + \lambda_2$. So, the increase in the amount of information from iteration $n = 0$ to iteration $n = 1$ is $\lambda_1 + \lambda_2$, which is H_{KS} calculated considering $l = 2$ in Eq. (16). Of course, if the spreading of points is uniform all over the space, and governed by the Lyapunov exponents, then $H_{KS} = \lambda_1 + \lambda_2$. If the spreading is not uniform, and governed by $P(i, j)$ depending on i and j , then one has $H_{KS} \leq \lambda_1 + \lambda_2$.

Assuming that a box of equal sides ϵ spreads out to the whole attractor Σ in an interval of time T is equivalent to stating that the interval $\sqrt{2}\epsilon$ is the largest side of the result of T backward iterations of the attractor Σ , and so $\epsilon\sqrt{2} = L \exp^{-\lambda_1 T}$, where L is the largest size of Σ . We are assuming that the attractor Σ is enclosed by an approximate rectangle, excluding some points that are located in the corners of the space Ω . The largest side of this rectangle is equal to $\epsilon\sqrt{2}\exp^{\lambda_1 T}$ whereas the second largest side is equal to $\epsilon\sqrt{2}\exp^{\lambda_2 T}$. The "area" of the attractor after a time T is $\epsilon^2 \exp^{(\lambda_1+\lambda_2)T}$. Considering two coupled 1D linear chaotic systems that are almost completely synchronous (Fig. 4(A)), this can be simply understood in terms of the BCLEs of this system. Assuming that the synchronization manifold is aligned to the direction that provides the largest Lyapunov exponent and BCLE, the more synchronous two coupled chaotic systems are the smaller are both the transverse conditional exponent $\lambda^{(2)}$ and the distance (approximately given by $\exp^{\lambda^{(2)T}}$) of points in the attractor to the synchronization manifold.

Now, we recall our definition of D as $D = \log(N_C)/\log(N)$, where $N = 1/\epsilon$. This definition is a

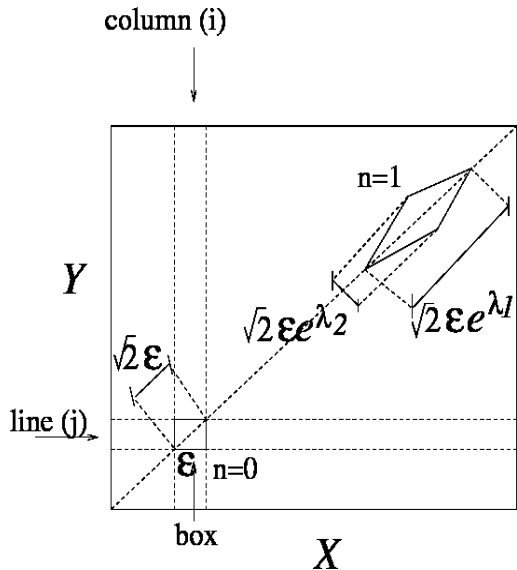


FIG. 2: A box with equal sides ϵ whose diagonal is placed along the diagonal line of the subspace Ω enclosing an area of ϵ^2 is iterated to a quadrilateral with an area of $\sqrt{2}/2\epsilon \exp^{\lambda_1} \times \sqrt{2}/2\epsilon \exp^{\lambda_2}$. At the iteration $n = 1$, there are $N_C = \frac{2\epsilon^2 \exp^{\lambda_1 + \lambda_2}}{\epsilon^2} = \exp^{(\lambda_1 + \lambda_2)}$ boxes.

consequence of the fact that $BN^D = N_C$ ($D \in [0, 2]$ and B representing a positive finite real number) and that N can be made arbitrarily large.

Let us now derive Eq. (2) (as well as the inequality in Eq. (3)). Recall that the phase space Ω is divided in N^2 boxes of side ϵ , and there are $\tilde{N}_C(\epsilon)$ boxes occupied by points in the set Σ . In addition, $N_C(T) = \tilde{N}_C(\epsilon)$, meaning that the points spread out uniformly according to the Lyapunov exponents and there are no fractal gaps in the set Σ when projected onto Ω . Recall that $P(i)$ is the probability of finding points in a column i , $P(j)$ of finding points in the line j , and $P(i, j)$ the probability of finding points in the box (i, j) . Whatever these probabilities are, if we consider that $P(i) = 1/N$ ($= \frac{1}{N_C} \frac{N_C}{N}$), $P(j) = 1/N$, and $P(i, j) = 1/N_C$, then the mutual information I_S obtained from it will be the maximal possible one. If the real probabilities $P(i), P(j)$, and $P(i, j)$ are different, then the mutual information, calculated using the real probabilities, would be smaller than the one calculated using that $P(i) = P(j) = 1/N$ and $P(i, j) = 1/N_C$.

A simple way to see that is by first assuming that points have already spread out during a time interval T . Then, notice that from Eqs. (4), (5), and (11), we have that $\tilde{N}_C \geq N_C$. In other words, the number of occupied boxes will be typically larger than the number of hypothetical boxes that would be occupied if the spreading of the points were governed by the expansion rate given by the Lyapunov exponents. Therefore, the mutual information, $I_S(\text{uniform, real})$, calculated assuming that

the boxes are uniformly occupied ($P(i) = P(j) = 1/N$ and $P(i, j) = 1/N_C$) is smaller or equal than the mutual information, $I_S(\text{uniform, hypothetical})$, calculated assuming that the hypothetical boxes are uniformly occupied ($P(i) = P(j) = 1/N$ and $P(i, j) = 1/N_C$). This later maximal mutual information is denoted by I_S^u , i.e., $I_S(\text{uniform, hypothetical}) = I_S^u$, a quantity from which we calculate I_C by $I_C = I_S^u/T$.

To make this explanation even more clear, assume again that points have already spread out during a time interval T . Assume also that only the boxes along the diagonal are occupied and that the frequency with which the hypothetical boxes are occupied equals the way the boxes are being occupied for real, which implies that after a time interval T we have that $N_C = \tilde{N}_C = N$. Assume additionally that during this expansion process, the boxes are occupied in a uniform fashion, and therefore, $P(i) = P(j) = P(i, i) = 1/N$. Under these conditions, the mutual information between systems X and Y is equal to the Shannon's entropy of system X (or Y), and therefore $I_S(\text{uniform, real}) = I_S(\text{uniform, hypothetical}) = \sum_i \frac{1}{P(i)} \log \left[\frac{1}{P(i)} \right] = \log(N)$. Finally, one would arrive to the conclusion that $I_C(\text{uniform, hypothetical}) = I_S(\text{uniform, real})/T$. Now, assume that the boxes are non-uniformly occupied, but still only the boxes along the diagonal are occupied and so $\tilde{N}_C = N_C$. Assume also that the boxes are symmetrically non-uniformly occupied, i.e., $P(i) = P(j)$ for $i = j$. The mutual information I_S between systems X and Y is again equal to the Shannon's entropy of system X (or Y) and then the mutual information calculated using the real non-uniform occupation of the boxes $I_S(\text{non-uniform, real})$ will be smaller or equal than the mutual information calculated using the uniform hypothetical occupation of the boxes $I_S(\text{uniform, hypothetical})$. This later maximal mutual information is denoted by I_S^u , i.e., $I_S(\text{uniform, hypothetical}) = I_S^u$, a quantity from which we calculate I_C by $I_C = I_S^u/T$.

In order to calculate I_S^u/T as a function of D , we insert $P(i)$ and $P(i, j)$ in Eq. (1), and assume, as discussed, that $D = \log(N_C)/\log(N)$. We arrive that the largest value that I_S can assume is

$$I_S^u = \log(N)(2 - D) \quad (17)$$

and

$$I_S^u \geq I_S. \quad (18)$$

So, I_S^u is an upper bound for I_S , where I_S in Eq. (18) represents the mutual information calculated using the real probabilities. The quantity I_S^u measures the amount of mutual information obtained after observing the system for an interval of time T . In order to calculate an upper bound for the MIR we have to divide I_S^u by T . Making the same assumptions as before, we get $\epsilon =$

$L/\sqrt{2} \exp^{-\lambda_1 T}$ and substituting $N = 1/\epsilon = \sqrt{2}/L \exp^{\lambda_1 T}$ in Eq. (17) yields

$$\frac{I_S^u}{T} = (2 - D) \left[\lambda_1 + \frac{1}{T} \log(\sqrt{2}/L) \right]. \quad (19)$$

But the term $\frac{1}{T} \log(\sqrt{2}/L)$ appearing in Eq. (19) can be ignored by making $\lim_{\epsilon \rightarrow 0}$, which implies $T \rightarrow \infty$, and therefore

$$I_C = \lambda_1(2 - D). \quad (20)$$

Let us now show that $I_C = I_S/T$ in Eq. (9). If $P(i, j)$ are constant for all i and j , then $I_C = I_S/T$, as in Eq. (9), since Eq. (19) is exactly the MIR (I_S/T) in case $P(i, j)$ is constant.

Another way to make the term $\frac{1}{T} \log(\sqrt{2}/L)$ to disappear from Eq. (19) is through a linear normalization of the set Σ by making $L = \sqrt{2}$. This linear normalization would allow the set Σ to fit in a square of sides 1, actually the “new” normalized subspace Ω . Notice that such a normalization does not change the values of λ_1, D and \tilde{D}_0 .

Let us now derive Eq. (10) and the conditions for which $I_C^l = I_S/T$ in Eq. (9). We assume that $\epsilon \rightarrow 0$ (recall that $\epsilon = 1/N$), and that the spreading of points is uniform only along columns and lines in the space Ω , i.e., $P(i) = P(j) = 1/N$ and $P(i, j)$ is not constant for all i and j . Under these conditions,

$$I_S(\epsilon) = -2 \log(\epsilon) + \sum_{i,j} P(i, j) \log[P(i, j)]. \quad (21)$$

Now, dividing $I_S(\epsilon)$ by $T(\epsilon) = -1/\lambda_1 \log(\epsilon)$, we arrive at

$$\frac{I_S(\epsilon)}{T(\epsilon)} = 2\lambda_1 + \frac{\lambda_1}{\log(\epsilon)} \sum_{i,j} P(i, j) \log[P(i, j)] \quad (22)$$

Taking the limit of $\epsilon \rightarrow 0$ and reminding that the information dimension of the attractor Σ in the space Ω is defined as

$$\tilde{D}_1 = \lim_{\epsilon \rightarrow 0} \frac{\sum_{i,j} P(i, j) \log[P(i, j)]}{\log(\epsilon)}, \quad (23)$$

substituting Eq. (23) in Eq. (22), we obtain that

$$I_S/T = \lambda_1(2 - \tilde{D}_1). \quad (24)$$

Also, once $\tilde{D}_1 \leq \tilde{D}_0$, then $\lambda_1(2 - \tilde{D}_1) \geq \lambda_1(2 - \tilde{D}_0)$, which means that $I_C^l \leq I_S/T$, as shown in Eq. (10). Finally notice that if $P(i, j) = 1/N_C$, then $\tilde{D}_1 = \tilde{D}_0$, implying that $I_S/T = I_C^l$, as in Eq. (8) and

$$I_S/T = \lambda_1(2 - \tilde{D}_0) \quad (25)$$

Using Eq. (25) and inequality in Eq. (5), we arrive at

$$I_C \geq I_S/T \quad (26)$$

B. The quantity D , Eq. (2), and inequality (5)

Now, let us show that Eq. (2) can be written in terms of the two largest positive Lyapunov exponents measured in the space Ω . This equation allows us to derive the upper bound proposed in Ref. [14] for the MIR in terms of the BCLEs, as discussed in Sec. III C. Again, one needs to use the fact that points in a given column (i) or line (j) will take $n = T$ iterations to spread all over the attractor Σ . For simplicity assume $L = \sqrt{2}$, which can always be set by making a linear normalization of the set Σ . Reminding also that $\epsilon = L/\sqrt{2} \exp^{-\lambda_1 T}$ and then for $L = \sqrt{2}$, we have that $N = \exp^{\lambda_1 T}$. As before, $P(i) = P(j) = 1/N = \exp^{-\lambda_1 T}$. As we have seen in the derivation of the KS entropy in terms of the Lyapunov exponents, the number of ϵ size boxes that fit Σ after a number T of iterations is given by $N_C(T) = \tilde{N}_C(\epsilon) = \exp^{(\lambda_1 + \lambda_2)T}$. The probability of finding a point in a box at the iteration T is $P(i, j) = 1/N_C = \exp^{-(\lambda_1 + \lambda_2)T}$. Substituting $P(i)$, $P(j)$ and $P(i, j)$ in Eq. (1), we obtain

$$I_S^u = 2T\lambda_1 - T(\lambda_1 + \lambda_2). \quad (27)$$

Upon dividing by T , we obtain an upper bound for the MIR

$$I_C = \lambda_1 - \lambda_2, \quad (28)$$

where λ_2 represents the second largest positive Lyapunov exponent measured on the subspace Ω . If the second largest exponent measured on the subspace Ω is negative, then Eq. (28) becomes $I_C = \lambda_1$.

Now, let us show that I_C in Eq. (2) is equal to I_C in Eq. (28). In order to do that, we calculate the quantity D in terms of the Lyapunov exponents. From the definition of D we have that $D = \frac{\log(N_C)}{\log(N)}$. Assuming as before that the size of the attractor is $L = \sqrt{2}$, and using that $N_C = \exp^{(\lambda_1 + \lambda_2)T}$ and $N = \exp^{\lambda_1 T}$, we get

$$D = 1 + \frac{\lambda_2}{\lambda_1}. \quad (29)$$

If the second largest exponent measured in the subspace Ω is negative, then $D = 1$.

D is defined in terms of positive Lyapunov exponents. It is different from the Kaplan-Yorke dimension, D_{KY} , (as well as the dimension D_a defined in [26] in terms of the expansion rates), that take into account also the negative Lyapunov exponents (negative expansion rates). Nevertheless, these quantities possess some similar properties. For example, it was conjectured that the Kaplan-Yorke dimension is an approximant for the information dimension, but it is smaller or equal than the capacity dimension. Similarly, $D \leq \tilde{D}_0$.

There is a simple way of understanding why $D \leq \tilde{D}_0$. Imagine two coupled 1D chaotic maps that have 2 positive Lyapunov exponents or the toy model presented in Sec. II C. One has that $D_{KY} = 2$, always, regardless

whether λ_2 (the second largest exponent) is very small or as large as λ_1 . But D can vary from 1 to 2, depending on the relative magnitudes of λ_1 and λ_2 . So, $D \leq D_{KY}$. Typically, for system that possess only positive Lyapunov exponents $D_{KY} \cong \tilde{D}_0$.

Another way for understanding why $D \leq \tilde{D}_0$ is by imagining a situation in which the attractor Σ (assumed to be a compact set, not a fractal) is not the whole space Ω . When we calculate D , as defined by Eq. (4), N is represented as a finite quantity, whereas in the definition of \tilde{D}_0 in Eq. (11), N is infinite (or ϵ can be made arbitrarily small). So, \tilde{D}_0 measures the changes in the number of occupied boxes as the space resolution varies, whereas D measures the relative number of (hypothetical) boxes at a certain fixed resolution N that would be occupied by points being iterated by a time T . As a consequence, the empty space in Ω that is not occupied by Σ does not contribute to the calculation of \tilde{D}_0 and then $\tilde{D}_0 = 2$, whereas it contributes to the calculation of the quantity D , resulting in $D < 2$.

Equation (28) which is completely equivalent to Eq. (2) is important because it relates the MIR with Lyapunov exponents and it can be of great help for analytical calculations. However, Eq. (6) can be more practical, since it relates the MIR with the capacity dimension, a widely used and known dynamical quantity. On the one hand, the quantity I_C^t might be closer to the “exact” value of the MIR (I_S/T), but to calculate \tilde{D}_0 one needs a large number of points.

To estimate the quantity \tilde{D}_0 appearing in Eq. (6), we consider a large N , but still finite, leading to

$$\tilde{D}_0 \approx \frac{\log(\tilde{N}_C)}{\log(N)} \quad (30)$$

with $N = 1/\epsilon$.

C. A dynamical toy model

To analytically demonstrate the relationship between I_C and I_S/T (Eq. (3)), we consider the following dynamical toy model illustrated in Fig. 3. In this dynamical toy model, points within a small box of sides ϵ in the center of the space Ω (represented by the filled square in Fig. 3(A)) are mapped after one iteration of the dynamics to 12 other neighboring boxes. Some points remain in the initial box. The points that leave the initial box go to 4 boxes along the diagonal line and 8 boxes off-diagonal along the transverse direction. Boxes along the diagonal are represented by the filled squares in Fig. 3(B) and off-diagonal boxes by filled circles. At the second iteration, the points occupy other neighboring boxes as illustrated in Fig. 3(C), and at the time $n = T$ the points do not spread any longer, but are somehow reinjected inside the region of the attractor.

At the iteration n , there will be $N_d = 2^{1+n} + 1$ boxes occupied along the diagonal (filled squares in Fig. 3) and

$N_t = 2nN_d - C(\tilde{n})$ (filled circles in Fig. 3) boxes occupied off-diagonal (along the transverse direction) where $C(\tilde{n}) = 0$ for $\tilde{n}=0$, and $C(\tilde{n}) > 0$ for $\tilde{n} \geq 1$ and $\tilde{n} = n - T - \alpha$, with α being a small number of iterations representing the time difference between the time T that the points in the diagonal reach the boundary of the space Ω and the time that the points in the off-diagonal reach this boundary. The border effect can be ignored when the expansion along the diagonal direction is much faster than along the transverse direction.

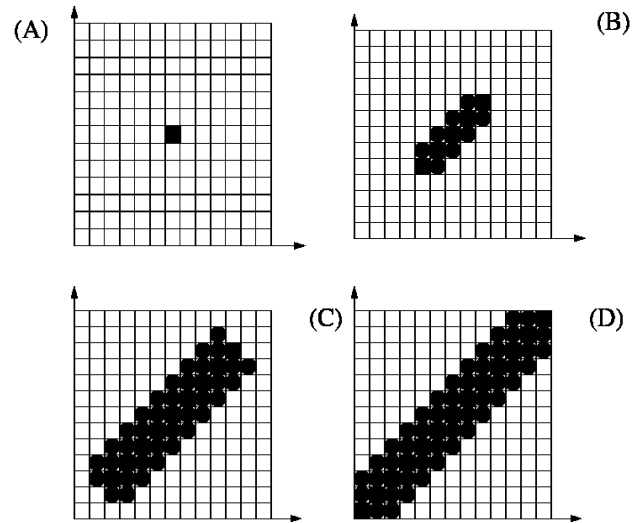


FIG. 3: (A) A small box representing a set of initial conditions. After one iteration of the dynamics, the points that leave the initial box in (A) go to 4 boxes along the diagonal line [filled squares in (B)] and 8 boxes off-diagonal (along the transverse direction) [filled circles in (B)]. At the second iteration, the points occupy other neighboring boxes as illustrated in (C) and after an interval of time $n = T$ the points do not spread any longer (D).

At the iteration n , there will be $N_C = 2^{1+n} + 1 + (2^{1+n} + 1)2n - C(\tilde{n})$ boxes occupied by points. In the following calculations we consider that $N_C \cong 2^{1+n}(1 + 2n)$. We assume that the space Ω is a square whose sides have length 1, and that $\Sigma \in \Omega$, so $L = \sqrt{2}$. For $n > T$, the attractor does not grow any longer along the off-diagonal direction. The time $n = T$, for the points to spread all over the attractor Σ , can be calculated by the time it takes for points to visit all the boxes along the diagonal. Thus, we need to satisfy $N_d \epsilon \sqrt{2} = \sqrt{2}$. Ignoring the 1 appearing in the expression for N_d due to the initial box in the estimation for the value of T , we arrive that $T > \frac{\log(1/\epsilon)}{\log(2)} - 1$. This dynamical model is discrete. In order to take into consideration the initial box in the calculation of T , we pick the first integer that is larger than $\frac{\log(1/\epsilon)}{\log(2)} - 1$, leading T to be the largest

integer that satisfies

$$T < -\frac{\log(\epsilon)}{\log(2)}. \quad (31)$$

The largest Lyapunov exponent of this toy model can be calculated by $N_d(n) \exp^{\lambda_1} = N_d(n+1)$, which take us to

$$\lambda_1 = \log(2). \quad (32)$$

Therefore, Eq. (31) can be rewritten as $T = -\frac{\log(\epsilon)}{\lambda_1}$, which is equal to Eq. (14).

The quantity D can be calculated by $D = \frac{\log(N_C)}{\log(N)}$, with $n = T$. Neglecting $C(\tilde{n})$ and the 1 appearing in N_C due to the initial box, we have that $N_C \cong 2^{1+T}[1 + 2^T]$. Substituting in the definition of D take us to $D = \frac{(1+T)\log(2) + \log(1+2^T)}{-\log(\epsilon)}$. Using T from Eq. (31), we arrive at

$$D = 1 + r, \quad (33)$$

where

$$r = -\frac{\log(2)}{\log(\epsilon)} - \frac{\log(1+2^T)}{\log(\epsilon)} \quad (34)$$

Placing D and λ_1 in Eq. (2), give us to

$$I_C = \log(2)(1 - r). \quad (35)$$

Let us now calculate I_S/T . Ignoring the border effect, and assuming that the expansion of points is uniform, then $P(i, j) = 1/N_C$ and $P(i) = P(j) = 1/N = \epsilon$. At the iteration $n = T$, we have that $I_S = -2\log(\epsilon) - \log(N_C)$. Since $N_C \cong 2^{1+T}[1 + 2^T]$, we can write that $I_S = -2\log(\epsilon) - (1+T)\log(2) - \log(1+2^T)$. Placing T from Eq. (31) into I_S takes us to $I_S = -\log(2) - \log(\epsilon) - \log(1+2^T)$. Finally, dividing I_S by T , we arrive that

$$\begin{aligned} \frac{I_S}{T} &= \log(2) \left[1 + \frac{\log(2)}{\log(\epsilon)} + \frac{\log(1+2^T)}{\log(\epsilon)} \right] \\ &= \log(2)(1 - r). \end{aligned} \quad (36)$$

As expected from the way we have constructed this model, Eq. (36) and (35) are equal and $I_C = \frac{I_S}{T}$.

Had we included the border effect in the calculation of I_C , denote the value by I_C^b , we would have typically obtained that $I_C^b \geq I_C$, since λ_2 calculated considering a finite space Ω would be either smaller or equal than the value obtained by neglecting the border effect. That is because nearby initial conditions diverge less along the off-diagonal at the border than away from the border. Had we included the border effect in the calculation of I_S/T , denote the value by I_S^b/T , typically we would expect that the probabilities $P(i, j)$ would not be constant. That is because the points that leave the space Ω would be randomly reinjected back to Ω . We would conclude

that $I_S^b/T \leq I_S/T$. Therefore, had we included the border effect, we would have obtained that $I_C^b \geq I_S^b/T$, verifying inequality (3).

The way we have constructed this dynamical toy model results in $D \cong 1$. This is because the spreading of initial conditions along the diagonal direction is much faster than the spreading of initial conditions along the off-diagonal transverse direction. In other words, the second largest Lyapunov exponent, λ_2 , is close to zero. To study toy models which produce larger λ_2 , one could consider that the spreading along the transverse direction is given by $N_t = N_d 2^{\alpha n} - C(\tilde{n})$, with $\alpha \in [0, 1]$.

III. TWO COUPLED PIECEWISE-LINEAR MAPS

Consider the following two bidirectionally coupled maps

$$\begin{aligned} X_{n+1}^{(1)} &= 2X_n^{(1)} + s\sigma(X_n^{(2)} - X_n^{(1)}), \text{ mod } 1 \\ X_{n+1}^{(2)} &= 2X_n^{(2)} + s\sigma(X_n^{(1)} - X_n^{(2)}), \text{ mod } 1, \end{aligned} \quad (37)$$

where $X \in [0, 1]$, $s = \pm 1$, $\sigma \leq 0.5$. For $\sigma = 0.5$, complete synchronization is achieved. The subspace Ω is a square of sides 1. As a consequence, the Lyapunov exponents measured in the subspace Ω are the Lyapunov exponents of the set Σ , the attractor generated by Eqs. (37).

The sign of s determines the level of synchronization and desynchronization that this coupled system has. If $s = -1$, this coupled system promotes the appearance of desynchronous trajectories. If $s = 1$, this coupled system promotes the appearance of synchronous trajectories. In Fig. 4 we show in (A) the trajectory for $s = 1$ and in (B) the trajectory for $s = -1$. For both figures, $\sigma = 0.4$. In (A), the trajectory points are close to the synchronization manifold defined by $\xi = X^{(1)} = X^{(2)}$ while in (B) one gets trajectory points aligned along the direction transverse to the synchronization manifold. The transverse direction can be calculated by $X^{(1)} + X^{(2)} = 1$.

A. Excitability and non-self-excitability of system in Eq. (37)

The Lyapunov exponents are $\log(2)$ and $\log(2[1 - 2s\sigma])$. In order to use our equations, λ_1 must always represent the largest lyapunov exponent, λ_2 the second largest and so on. If $s = 1$, $\lambda_1 = \log(2)$ and $\lambda_2 = \log(2[1 - 2\sigma])$. If $s = -1$ then $\lambda_1 = \log(2[1 + 2\sigma])$ and $\lambda_2 = \log(2)$.

If $s = 1$, as one increases the coupling strength σ the sum of the Lyapunov exponents, denoted by H_{KS} (an upper bound or equal to the KS-entropy [9–11]), decreases. If $s = -1$, as one increases the coupling strength σ , H_{KS} increases.

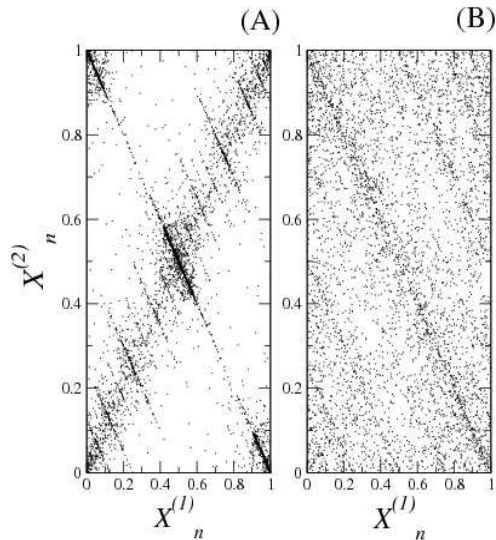


FIG. 4: Chaotic attractors of Eq. (37) for $s = 1$ (A) and $s = -1$ (B).

In Ref. [14] we have proposed a classification of networks as a way to relate the coupling strength and an upper bound for the MIR. We have classified a network to be non-self-excitable (NSE) if I_C between two nodes becomes smaller than H_{KS}^0 as one varies the coupling strength within some interval. H_{KS}^0 represents the KS entropy of an uncoupled node. A network is said to be self-excitable (SE) if I_C between two nodes is equal or larger than H_{KS}^0 as one varies the coupling strength within some interval. For the coupled maps of Eqs. (37), $H_{KS}^0 = \log(2)$.

It is not difficult to check that for both cases, $s = 1$ and $s = -1$, one has a non-self-excitable coupled map for $\sigma \in]0, 0.5[$, since using Eq. (28), $I_C = -s \log(1 - 2s\sigma)$ and so $I_C < \log(2)$. In other words, for such a coupled system, the coupling does not cause the two systems to exchange more information than the information each map produces when isolated from the network.

B. Synchronization vs. MIR

If $s = 1$, λ_1 is not only the largest Lyapunov exponent but is also equal to the Lyapunov exponent, $\lambda^{(1)}$, along the synchronization manifold, and λ_2 is not only the second largest Lyapunov exponent but is also equal to the Lyapunov exponent, $\lambda^{(2)}$, calculated along the transverse direction to the synchronization manifold. If $s = -1$, $\lambda_1 = \lambda^{(2)}$ and $\lambda_2 = \lambda^{(1)}$. The Lyapunov exponents along the synchronization manifold and the direction transverse to the synchronization manifold were called B-conditional lyapunov exponents (BCLEs), see Ref. [16]. They are in general not equal to the Lyapunov

exponents. But since Eq. (37) has a constant Jacobian, the Lyapunov exponents are equal to the B-conditional lyapunov exponents.

This system of coupled maps provides an ideal condition to understand the relationship between the MIR and the level of synchronization. That is so, because the larger $\lambda^{(2)}$ is, the more desynchronous the two coupled systems are. If $s = -1$, the amount of information produced by the desynchronous trajectories ($\lambda_1 = \lambda^{(2)}$) is larger than the amount of information produced by the synchronous trajectories. But even when the level of desynchronization is high, and $\lambda^{(2)} > \lambda^{(1)}$, information can still be transferred from one system to the other. This counter-intuitive result, numerically verified in Ref. [15], was explained by conjecturing (based on physical arguments) that when $\lambda^{(2)} > \lambda^{(1)}$, then $I_C = \lambda^{(2)} - \lambda^{(1)}$, a conjecture that we will show in the next section to be verified. However, notice that $I_C(s = 1) \leq I_C(s = -1)$. That means that synchronous states provide better conditions for the exchange of information than desynchronous states.

C. Upper and lower bounds for the MIR

The upper bound for the MIR derived in Refs. [14, 15] states that the MIR between the maps in Eq. (37) must be smaller than or equal to $\lambda^{(1)} - \lambda^{(2)}$, where $\lambda^{(1)}$ and $\lambda^{(2)}$ are the two largest BCLEs of Eq. (37). From now on, $\lambda^{(1)}$ denotes the largest BCLE. The calculation of the largest exponent is made not necessarily along the direction of the synchronization manifold. So, we organize the BCLEs according to their absolute value, i.e., $\lambda^{(1)} > \lambda^{(2)}$. For Eqs. (37), with $s=1$, we have that $\lambda^{(1)} = \lambda_1$ and $\lambda^{(2)} = \lambda_2$. Therefore, Eq. (28) can be written in terms of the conditional exponents as $\lambda^{(1)} - \lambda^{(2)}$, as conjectured in Refs. [14, 15].

Let us now compare the values of our upper and lower bounds coming from Eqs. (2) and Eq. (6), respectively, with the estimated “exact” value of the MIR, I_S/T , given by the right-hand side of Eq. (3). We calculate I_S using in Eq. (1) the probabilities $P(i, j)$ in which points from a trajectory composed of 2,000,000 samples fall in boxes of sides $\epsilon = 1/500$ and the probabilities $P(i)$ and $P(j)$ that the points visit the intervals $[(i-1)\epsilon, i\epsilon[$ or $[(j-1)\epsilon, j\epsilon[$, respectively, for $i, j = 1, \dots, N$. The largest size L of the attractor appearing in Eq. (14) is $\sqrt{2}$. When computing I_S/T , the quantity T was estimated by Eq. (14).

These quantities are shown in Fig. 5 as we vary σ for $s = 1$ (A) and $s = -1$ (B). We show I_S/T as (green online) filled circles, I_C [Eq. (28)] as the (red online) thick line, and I_C^l [Eq. (6), using \tilde{D}_0 as calculated by Eq. (30)] as the (brown online) crosses. Indeed for most cases $I_C \geq I_S/T$ and $I_C^l \leq I_S/T$.

There are two coupling strengths which are interesting to discuss the performance of the proposed bounds for the MIR and the quantity I_S/T . For $\sigma = 0$ there is no coupling. As usually happens when one estimates

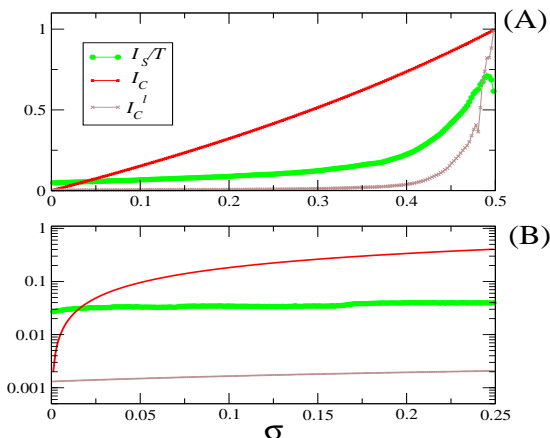


FIG. 5: [Color online] I_S/T as (green online) filled circles, I_C [Eq. (28)] as the (red online) thick line, I_C^l [Eq. (6), using \tilde{D}_0 as calculated by Eq. (30)] as the (brown online) crosses. In (A), $s = 1$ and in (B) $s = -1$. In (B), because both I_S/T and I_C^l are small, we use a log-axis. The units of I_S/T , I_C , and I_C^l are [bits/iteration], which means that we are plotting these quantities divided by $\log(2)$.

the mutual information by partitioning the phase space in boxes using a finite number of samples, I_S is typically larger than zero, even when there is no information being exchanged. For this system of coupled maps, the lower bound I_C^l suffers from the same problem. As a consequence, any estimation of mutual information for finite resolution of the grid and a finite number of points would arrive to a positive and far from zero mutual information. On the other hand, the upper bound I_C is null when there is no coupling, as one should expect.

For $\sigma \rightarrow 0.5$ and $s = 1$, in Fig. 5(A), complete synchronization sets in. As a consequence, $D = \tilde{D}_0 = 1$, and therefore, $I_C = I_C^l = \lambda_1$, as it has to be. The quantity I_S/T is close to this value, but smaller. The reason for this discrepancy is again the finiteness of the boxes. Even when there is complete synchronization, we find non-zero off-diagonal terms in the matrix for the joint probabilities ($P(i, j) \neq 0$, for $i \neq j$), causing the mutual information to be smaller than it should be. In fact, there will be approximately $2N$ off-diagonal boxes containing points causing the estimated value of I_S to be underestimated.

Notice that in Fig. 5(A) for $s=1$, Eq. (9) is partially verified for $\sigma = 0$ and $\sigma = 0.5$. The reason is that for these coupling strengths, the coupled system is just the shift map, a map with constant natural measure and therefore $P(i) = P(j)$ and $P(i, j)$ is constant for all i and j . Additionally, for these coupling strengths, D assumes integer values: $D=2$ for $\sigma = 0$ and $D=1$ for $\sigma = 0.5$. But, when $D=2$ we have that $D_0 = 2$ as well, since the

attractor Σ fully occupies the subspace Ω .

For $\sigma \in [0.1, 0.48]$, our upper bound is larger than I_S/T . The reason is because for such σ values, this coupled map becomes strongly non-uniform. Regions close to the points $(0, 0)$, $(0, 1)$, $(1, 0)$, $(1, 1)$ have a large probability density, while other regions have small probability density. As a consequence the probabilities $P(i, j)$ for the occupancy of the boxes are highly non-uniform. In the derivation of the upper bound, we assume that the spreading of the points is uniform.

We would like to point out that one of the main advantages of calculating upper bounds for the “exact” MIR (I_S/T) using Eqs. (2) or (28) instead of actually calculating I_S/T is that we can reproduce the curves for I_C using much less points (1000 points) than the number of points (2,000,000) used to calculate the curve for I_S/T .

IV. TWO COUPLED NON-LINEAR MAPS

As previously discussed, we have proposed a conjecture [13, 14] that states that an upper bound for the mutual information rate between two systems within a network of chaotic systems can be calculated by

$$I_C^u = \lambda^{(1)} - \lambda^{(2)} \quad (38)$$

Let us consider the following system of coupled maps,

$$\begin{aligned} X_{n+1}^{(1)} &= 2X_n^{(1)} + \rho X_n^{(1)^2} + \sigma(X_n^{(2)} - X_n^{(1)}), \text{ mod } 1 \\ X_{n+1}^{(2)} &= 2X_n^{(2)} + \rho X_n^{(2)^2} + \sigma(X_n^{(1)} - X_n^{(2)}), \text{ mod } 1 \end{aligned} \quad (39)$$

where $X \in [0, 1]$. When $\rho = 0$, system (39) is equal to system (37) and the Jacobian is constant. As a consequence $\lambda^i = \lambda_i$ and thus $I_C^u = I_C$. When $\rho \neq 0$, the conditional exponents, $\lambda^{(1)}$ and $\lambda^{(2)}$, are slightly different than the Lyapunov exponents, λ_1 and λ_2 , offering us an ideal situation to compare the conjecture in Eq. (38) with Eq. (28). The subspace Ω is a square of sides 1. As a result, the Lyapunov exponents measured in the subspace Ω are the Lyapunov exponents of the set Σ , the attractor generated by Eqs. (39).

In Fig. 6, we show the estimated “exact” value of the MIR, I_S/T , given by the right-hand side of Eq. (3), I_C in Eq. (2), I_C^l as defined in Eq. (6), and I_C^u as defined in Eq. (38) for $\rho=0.1$ (A) and $\rho=-0.1$ (B). I_S is calculated using the same grid described in Sec. III C. As one can see, $I_C \cong I_C^u$. That is because ρ is small and the BCLEs are close to the Lyapunov exponents. Besides, I_C as well as I_C^u are both upper bounds for the MIR provided by I_S/T , except for when $\sigma \cong 0$. There, $I_C < I_S/T$ and $I_C^u < I_S/T$, but this is, as discussed in the previous section, an artifact since we do not have an infinite trajectory and the phase space is not being divided in an infinite number of boxes.

The difference between I_C and I_C^u is that for most of the coupling strength considered, $I_C > I_C^u$ for $\rho=0.1$, in (A) and $I_C < I_C^u$ for $\rho=-0.1$, in (B). This might be a consequence of the conjecture proposed in Ref. [19]

that states that for this two coupled system, $\lambda_1 + \lambda_2 < \lambda^{(1)} + \lambda^{(2)}$ if $\rho=0.1$ and that $\lambda_1 + \lambda_2 > \lambda^{(1)} + \lambda^{(2)}$ if $\rho=-0.1$. Since for this coupled system $\lambda_1 \cong \lambda^{(1)}$, it is to be expected that $I_C > I_C^u$ for $\rho=0.1$ in (A) and $I_C < I_C^u$ for $\rho=-0.1$ in (B).

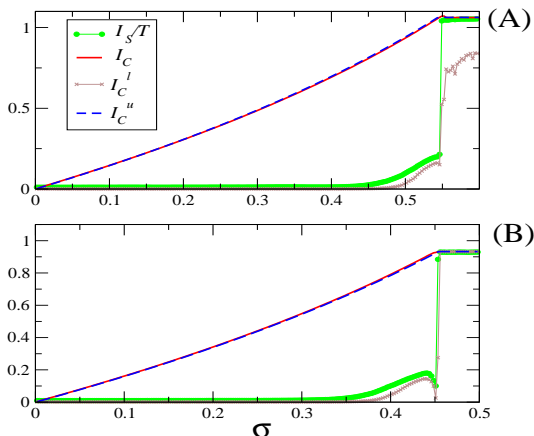


FIG. 6: [Color online] I_S/T as (green online) filled circles, I_C [Eq. (28)] as the (red online) thick line, I_C^l [Eq. (6), using \tilde{D}_0 as calculated by Eq. (30)] as the (brown online) cross, and I_C^u [Eq. (38)] as the (blue online) dashed line. In (A), $\rho = 0.1$ and in (B) $\rho = -0.1$. The units of I_C and I_S/T are [bits/iteration], which means that we are plotting these quantities divided by $\log(2)$.

If the sign of ρ is positive (Fig. 6(A)), these two coupled maps become completely synchronous for a coupling strength σ larger than the strength one would need to use to achieve complete synchronization when the sign of ρ is negative (Fig. 6(B)). When complete synchronization is achieved, I_C , I_C^l , I_C^u , and I_S/T take their maximal values. The values of these quantities for a given value of the coupling strength σ are larger when $\rho > 0$ than when $\rho < 0$. Therefore, if the non-linear term $\rho X_n^{(i)2}$ is negative it acts in an inhibitory fashion decreasing the MIR between the coupled maps. This non-linear term can be interpreted as a dynamical noise which prevents both maps to exchange information.

Finally, notice that for $\sigma = 0$ and for σ leading to complete synchronization, Eq. (9) is almost satisfied because of the same reasons described in the previous section.

V. EXPANSION RATES

For the treatment of data sets coming from networks whose equations of motion are unknown, or for higher-dimensional networks, we can extend our approach as

long as the network has deterministic characteristics, as in **definition 1**, if one can calculate expansion rates, defined as in the following.

The expansion rates we define in this work are similar to the finite-time Lyapunov exponents (FTLEs) [27, 28], in the sense that our expansion rates measure the exponential divergence of nearby points for a finite interval of time. However, it differs from the FTLEs because we consider finite sized regions and an interval of time much smaller than the one used to calculate the FTLEs. Our expansion rates are also similar to the expansion rates defined in Ref. [26, 29, 30], because in those works finite regions and a finite small interval of time are being considered. However, the expansion rates defined in this work are the local Lyapunov exponent of finite regions for a well defined finite time interval T , whereas the expansion rates defined in Ref. [26] are the logarithm of the average expansion of arbitrarily small regions for some finite interval of time. In Sec. V A we will explain all the 4 reasons behind our definition. One of the reasons is because we want to have a measure that is appropriated to complex data sets where Lyapunov exponents or expansion rates as rigorously defined are difficult or virtually impossible to be estimated.

Let us define $L_k^i(t)$ as the ratio with which points inside a k -dimensional hypercube i spread out for an interval of time t . Then, an order- k expansion rate is defined in Ref. [26] as $E_k(t) = 1/q \sum_i L_k^i(t)$, with the average being taken considering $i = 1, \dots, q$ regions. As a consequence of this definition, one can argue that $\log(E_k) \leq \sum_i^k \lambda_i$.

We define expansion rates as

$$e_k(t) = 1/q \sum_{i=1}^q \log[L_k^i(t)]. \quad (40)$$

If the Jacobian of the system is constant everywhere and the spreading of points is uniform everywhere, we can set $t = T$, otherwise if there are not enough points in the data set, or the spreading of points is highly non-uniform, we consider $t < T$ in the estimation of e_k . In Sec. V C we will discuss which value of t must be chosen in order to calculate physically consistent expansion rates. Typically, t is such that points initially in a small box spread out to a significant portion of the attractor.

An order- k expansion rate, $e_k(t)$, measures on average how a hypercube of dimension k exponentially grows after an interval of time t . So, e_1 measures the largest growth rate of nearby points, a quantity closely related to the largest finite-time Lyapunov exponent. And e_2 measures how an area enclosing points grows.

In terms of expansion rates, Eqs. (2) and (14) read

$$I_C = e_1(2 - D), \quad (41)$$

and

$$T \approx \frac{1}{e_1} \log \left[\frac{L}{\epsilon} \right], \quad (42)$$

and Eq. (4) and (6) read

$$D(t) = \frac{e_2(t)}{e_1(t)}, \quad (43)$$

and

$$I_C^l = e_1(2 - \tilde{D}_0). \quad (44)$$

A. Expansion rates vs. Lyapunov exponents

As argued in Ref. [26], an order- k expansion rate as defined in that work, differs from $\sum_i^k \lambda_i$. Our expansion rates behave similarly, i.e., typically $e_k \neq \sum_i^k \lambda_i$. These two quantities are equal when the Jacobian of the system is constant. The difference between Lyapunov exponents and expansion rates appears because the Lyapunov exponents are microscopic quantities, locally calculated, whereas the expansion rates are macroscopic quantities, globally calculated. In the one hand, Lyapunov exponents measure on average how arbitrarily small neighborhoods of points grow after an arbitrarily small time interval. In the other hand, expansion rates, as defined in this work, measure how points within a finite region spread out through significant portions of the attractor after a finite time interval $t \cong T$.

How much expansion rates (considering all the definitions) differ from Lyapunov exponents is an open problem that has been given very few attention lately, despite the fact that expansion rates (including FTLEs) are a convenient way to study and analyze complex systems. There are many reasons for using expansion rates in the way we have defined them in order to calculate bounds for the MIR. Firstly, because they can be easily experimentally estimated whereas Lyapunov exponents demand huge computational efforts [26]. Secondly, because of the macroscopic nature of the expansion rates, they might be more appropriate to treat data coming from complex systems, data that have points that are not (arbitrarily) close as formally required for a proper calculation of the Lyapunov exponents. Thirdly, expansion rates can be well defined for data sets containing very few data points: the fewer points a data set contains, the larger the regions of size ϵ need to be and the shorter the time t is. Finally, expansion rates are defined in a similar way to finite-time Lyapunov exponents and thus some algorithms used to calculate Lyapunov exponents can be used to calculate our defined expansion rates.

From the way we have defined expansion rates, we expect that $e_k \leq \sum_{i=1}^k \lambda_i$ ([31, 32]). Because of the finite time interval and the finite size of the regions of points considered, regions of points that present large derivative and that would contribute largely to the Lyapunov exponents, contribute less to the expansion rates.

To illustrate why $e_k \leq \sum_i^k \lambda_i$, in Fig. 7, we compare the Lyapunov exponents with the order-1 expansion rate

for the Logistic map ($X_{n+1} = 4X_n * (1 - X_n)$), using the algorithm described in the next section (Sec. VB), considering different intervals ϵ , a trajectory with 10,000,000 points, and assuming that

$$t = T = -\frac{1}{\log(2)} \log(\epsilon). \quad (45)$$

In fact, $e_1 < \lambda_1$, where $\lambda_1 = \log(2)$. As a consequence, in the following results, one should bare in mind that I_C calculated from Eq. (2) should be slightly larger than I_C calculated from Eq. (41), and T calculated from Eq. (14) should be slightly smaller than when calculated by Eq. (42). All these inequalities lead one to the conclusion that I_S/T using T calculated from Eq. (14) should be slightly smaller than I_S/T using T calculated from Eq. (42). Therefore, I_S/T and I_C calculated using the expansion rates are both also slightly smaller and, as a result, inequality (3) is satisfied regardless whether one uses Lyapunov exponents or expansion rates.

Let us try to understand that. Assume first that the same conditions to derive Eq. (25) applies. Writing this equation in terms of the expansion rates we have that $I_S/T = e_1(2 - \tilde{D}_0)$. And we have that $I_C = e_1(2 - D)$. Using inequality in Eq. (5) we see that $I_S/T \leq I_C$. Assume now that the same conditions to derive Eq. (24) applies. Writing this equation in terms of the expansion rates we have that $I_S/T = e_1(2 - \tilde{D}_1)$. For the same reasons that condition (5) are constructed, we expect to have that $\tilde{D}_1 \geq D$. So, again $I_S/T \leq I_C$.

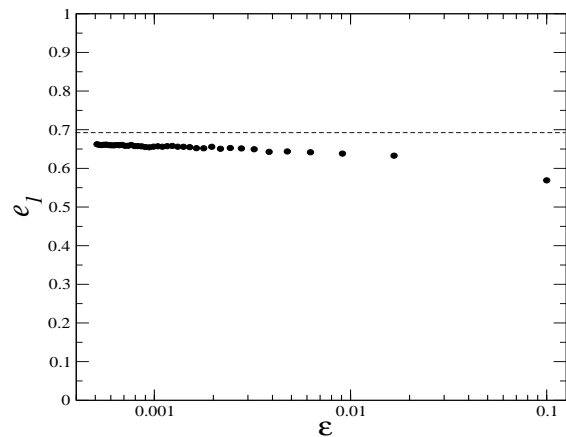


FIG. 7: [Color online] Order-1 expansion rate e_1 for the Logistic map with respect to the interval ϵ . The dashed line represents the value of the Lyapunov exponent of the Logistic map, $\lambda_1 = \log(2)$.

From the previous arguments, the values of I_C and I_S/T calculated using the Lyapunov exponents is higher

than if one considers expansion rates. That is a consequence of the fact that in the calculation of the Lyapunov exponents one can capture more information about the dynamics of the systems than the amount one would obtain in the calculation of expansion rates. That is a direct consequence of the fact that the expansion rates, as defined in here, “filters out” the existence of regions of points with large local expansion rates. However, the largest possible value for I_C is obtained when one considers in the calculation of I_C the Lyapunov exponents.

As one can check in Fig. 7, the expansion rate can be close to the Lyapunov exponent, i.e., $e_1 \cong \lambda_1$. The same happens to the finite-time Lyapunov exponent whose probability distribution is centered around the Lyapunov exponent [28]. Since the Logistic map has dynamical properties very similar to the systems considered in this work, in the following we will assume that

$$e_k \cong \sum_i^k \lambda_i \quad (46)$$

If we had defined expansion rates considering the averaged logarithm of the local expansion of finite regions within an interval of time considerably smaller than T , our order-1 expansion rate would be defined in a similar way to the finite-size Lyapunov exponent defined in Ref. [33]. For sufficiently small finite size regions, the exponent defined in Ref. [33] approach the largest Lyapunov exponent. This fact also supports Eq. (46)

B. Algorithm to calculate expansion rates

Let us introduce the algorithm we use to calculate expansion rates. Assume two discrete data sets $\mathcal{X} = X_1, X_2, \dots, X_k$ and $\mathcal{Y} = Y_1, Y_2, \dots, Y_k$ containing each k points. We assume that X_i is measured simultaneously to Y_i . After projecting these two data sets into the subspace Ω , in this subspace expansion rates [26] can be defined by measuring how nearby points exponentially diverge.

Assume that the sampling time rate is δ . The k data points are represented by $\mathcal{X} = X(0), X(\delta), \dots, X(k\delta)$ and $\mathcal{Y} = Y(0), Y(\delta), \dots, Y(k\delta)$. To simplify the notation we consider that a point of the data set \mathcal{X} collected at the time $i\delta$ can be represented by X_i . The space Ω is constructed by plotting in the horizontal axis the points X_i and in the vertical axis the points Y_i .

Linear normalization of the space Ω does not alter λ_k as well as e_k , D and \tilde{D}_0 . Therefore, we normalize the set Σ such that $X_i \in [0, 1]$ and $Y_i \in [0, 1]$. As a consequence, the subspace Ω is a square of sides 1. This normalization allows us to coarse grain the subspace Ω in a grid of boxes of equal sides ϵ .

We then calculate the order-1 expansion rate in the following way. Let us call each box $C^{(i,j)}$ (with $i, j = 1, N$). The box $C^{(i,j)}$ is defined by $[\epsilon(i-1), \epsilon i] \times [\epsilon(j-1), \epsilon j]$, $(i, j) = (1, \dots, N)$.

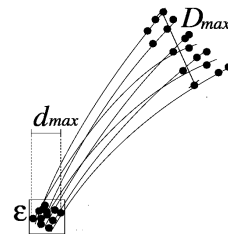


FIG. 8: In the ϵ size box the maximal distance between pairs of points is represented by d_{max} . The points initially inside the box spread out to a larger area of points after a time $t = q\delta$. The maximal distance between points in the iterated set of points is represented by D_{max} . Notice that the maximal distance between pair of points inside a box might be different than the diagonal of the box.

For each box $C^{(i,j)}$, we search for points (X_{k_i}, Y_{k_i}) that belong to it and we choose a time

$$t = q\delta, \quad (47)$$

q times the sampling time rate such that the set composed by the time evolution of the points (X_{k_i}, Y_{k_i}) , represented by $F^t(X_{k_i}, Y_{k_i})$, occupies a significant region of the attractor Σ . By significant region we mean that we try as much as possible to satisfy the conditions described in the next section.

We only take into consideration boxes that contain a minimal number of points, N_0 . Let us say that there are \tilde{n}_C such boxes and these boxes are denoted by $\tilde{C}^{(i,j)}$. That is a necessary requirement, since $e_2(t)$ is calculated from \tilde{n}_C . When the number of points inside a box is smaller than the number of boxes that would be visited by the iterated points $F^t(X_{k_i}, Y_{k_i})$ (if the data set had an infinite amount of points), then e_2 will be underestimated because \tilde{n}_C observed will be smaller than the value one would observe (if the data set had an infinite amount of points).

We measure the maximal distance between all pairs of points that are inside the box $\tilde{C}^{(i,j)}$, and denote it by $d_{max}^{(i,j)}$. We also measure the maximal distance between all pairs of points in $F^t(X_{k_i}, Y_{k_i})$, and denote it by $D_{max}^{(i,j)}$. The order-1 local expansion rate $e_1^{(i,j)}$ for the box \tilde{C}_{ij} can be estimated by

$$e_1^{(i,j)} = \frac{1}{t} \log \left[\frac{D_{ij}^{max}}{d_{ij}^{max}} \right]. \quad (48)$$

Figure 8 illustrates the definition of d_{max} and D_{max} . We consider that $t \leq T$, meaning that the points in the iterated set $(F^t(X_{k_i}, Y_{k_i}))$ visit a significant portion of the attractor Σ . The averaged order-1 expansion rate e_1 can be calculated by

$$e_1(t) = \frac{1}{\tilde{n}_C} \sum_{i,j} e_1^{(i,j)}. \quad (49)$$

To calculate the averaged order-2 expansion rate, e_2 , we need to measure the quantity $\tilde{N}_C(t)^{(i,j)}$. This quan-

tity represents the local number of boxes that points initially in a box \tilde{C}_{ij} visit after being iterated for a time t . Then, we should have that

$$\tilde{N}_C(t)^{(i,j)} = \exp^{e_2^{(i,j)} t} \quad (50)$$

and, therefore,

$$e_2^{(i,j)} = \frac{\log(\tilde{N}_C(t)^{(i,j)})}{t}. \quad (51)$$

Then, averaging over all the \tilde{n}_C boxes we obtain that

$$e_2(t) = \frac{1}{\tilde{n}_C} \sum_{i,j} e_2^{(i,j)}. \quad (52)$$

C. Which ϵ and t to choose?

The quantities λ_i , D , D_0 , e_i can each be calculated using regions defined in different ways. Some algorithms, as in Refs. [34, 35], propose to calculate λ_1 using regions defined in a way to contain a maximal number of points. The size of the regions may vary. A similar procedure is employed in Ref. [25] to calculate I_S . From the way the capacity dimension is defined [36], \tilde{D}_0 is calculated using boxes with equal sides. In this work, we want to compare I_S , I_C , and I_C^l , which are functions of these quantities. In order to be able to calculate all these quantities using the same regions and also to be consistent with the way we have done our theoretical derivations, we will consider in the calculation of these quantities boxes of equal sides chosen according to the following rules.

We first assume that the data sets considered here possess deterministic properties as in definition 1. Testing whether the data possess such a property is a way to define the optimal value of ϵ and the interval of time t considered to calculate the expansion rates. Let us define $N_C(T, e_2)$ as the hypothetical number of boxes that would be visited after a time interval T in case points spread out according to $e_2(t)$. So, this fictional number of boxes can be estimated by

$$N_C(T, e_2) = \exp^{T e_2(t)}, \quad (53)$$

where $e_2(t)$ is calculated by Eq. (52).

We consider the optimal ϵ and t as the following:

- (i) $N_C(T, e_2)$ is of the same order of magnitude of the number of occupied boxes, so

$$N_C(T, e_2) \cong \tilde{N}_C(\epsilon), \quad (54)$$

T is estimated from Eq. (42), using the value of ϵ representing the sides of the boxes and $e_2(t)$ is calculated considering a time interval t , with $t \leq T$. In a more friendly language, we require that the expansion rate $e_2(t)$ describes well the way points really spread. For further use, we define the quantity

$$r = |N_C(T, e_2) - \tilde{N}_C(\epsilon)|. \quad (55)$$

We choose ϵ and t in order to minimize r .

- (ii) In order to be able to well estimate e_2 , we require that boxes must contain a sufficient amount of points. Let us denote $N_0^{(i,j)}$ as the number of initial points in each (i, j) box. To well estimate the local expansion rates $e_2^{(i,j)}$ it is required that $N_0^{(i,j)}$ is of the order or larger than the number of occupied boxes \tilde{N}_C . So, we require that $N_0^{(i,j)} \geq \tilde{N}_C$. In practice, we do not check this condition for each box, but only on an average sense, i.e., we require that

$$\langle N_0(\epsilon) \rangle \geq \tilde{N}_C, \quad (56)$$

where $\langle N_0 \rangle$ is the average number of initial points inside boxes with sides ϵ .

D. Condition (i) and e_2 for data sets

When dealing with data sets that contain a finite number of points and with grids that contain a finite number of boxes with a finite ϵ precision, the quantity $\tilde{N}_C(\epsilon)$ in condition (i) in Sec. V C is set to be equal to

$$\tilde{N}_C(\epsilon) = \tilde{N}_C(\epsilon) - 2N. \quad (57)$$

The $2N$ appearing in this equation is due to the finiteness of the boxes and the experimental resolution and level of noise. Assume that the circuits are completely synchronous and there is no experimental noise. The points will be along a 1-dimensional line. If there is noise and the boxes have a finite size the points will not be perfectly positioned along the diagonal line, but they will be spreaded around this line. One would obtain that $\tilde{N}_C(\epsilon) = 3N$, but one should actually have obtained $\tilde{N}_C(\epsilon) = N$.

Since the points do not completely occupy the initial box, Eq. (51) should be rewritten. This equation was constructed assuming that a box of sides ϵ with an area ϵ^2 grows after an interval of time t to an "area" given by $\tilde{N}_C(t)^{(i,j)} \epsilon^2$. But actually, the effective area of the initial box \tilde{C}_{ij} is not ϵ^2 , but

$$\epsilon' = \frac{d_{ij}^{max}}{\sqrt{2}}, \quad (58)$$

assuming that d_{ij}^{max} is the diagonal of the effective box covering the initial points with equal sides ϵ' .

Then, Eq. (50) should be rewritten as

$$\tilde{N}_C = \epsilon' \exp^{e_2^{(i,j)} t},$$

which take us to

$$e_2^{(i,j)} = \frac{1}{t} \log \left(\frac{\sqrt{2} \tilde{N}_C(t)^{(i,j)}}{d_{ij}^{max}} \right). \quad (59)$$

VI. A NETWORK OF EXPERIMENTAL CHUA'S CIRCUIT

The Chua's circuit [37] is one of the simplest autonomous known circuits that can generate chaos. An usual Chua's circuit contains 2 capacitors, one inductor, and a nonlinear component that has a piecewise-linear response curve. The circuit used in this work is an inductorless version of the original circuit [38].

Even though the experimental circuit has three state variables, only one was acquired. Naturally, one could construct the 2D space Ω by making a Poincaré map of a higher dimensional reconstructed trajectory using time-delay coordinates from the two measurable variables, \mathcal{X} and \mathcal{Y} . One could then calculate the expansion rates using the points of this mapping. In this section, we want to give an example of how to calculate bounds for the MIR using a subspace that is trivial to be constructed (without time-delay embedding). A subspace Ω constructed considering that one axis represents the continuous variable \mathcal{X} and in the other axis the continuous variable \mathcal{Y} . In this way, we obviously maximize the number of points on the space Ω . Additionally, not being necessary to employ time-delay reconstruction techniques might simplify the computational efforts to analyze the data and does not require attention concerning the existence of spurious Lyapunov exponents, which only appear as a consequence of the embedding.

We consider 4 networks of mutually diffusively coupled Chua's circuit as presented in Fig. 9. We collect from each circuit a set of 79980 points, with a sampling rate of $\delta = 80.000\text{samples/s}$. The measured variable is the voltage across one of the Chua's circuit capacitors, that we represent by X_i , $i = 1, \dots, 4$.

A. Treating the data

To treat all the data sets obtained from the experimental networks of Chua's oscillator, we vary N and t in order to satisfy the conditions in Sec. V C. We consider $N \in [10, N_{max}]$ and $t \in [2\delta, t_{max}]$, where N_{max} is the value of N for which condition (56) is no longer satisfied and t_{max} is the maximal averaged time interval needed for two nearby points in an initial box (average taken by considering all occupied boxes) to become $0.75 * L$ apart. In other words, points inside a typical box will visit 75% of the attractor when iterated by a time t_{max} . This percentage of 75% was chosen to guarantee that in our estimate of the expansion rates, initially nearby points will be on average spreading exponentially, and that $t \approx T$. If we had chosen 99%, while some points initially close would exponentially diverge even after becoming 99% of the attractor size apart, some others would be approaching themselves.

To save computing time, we consider that condition (54) is satisfied when $r < 0.01$ and if e_1 , estimated when

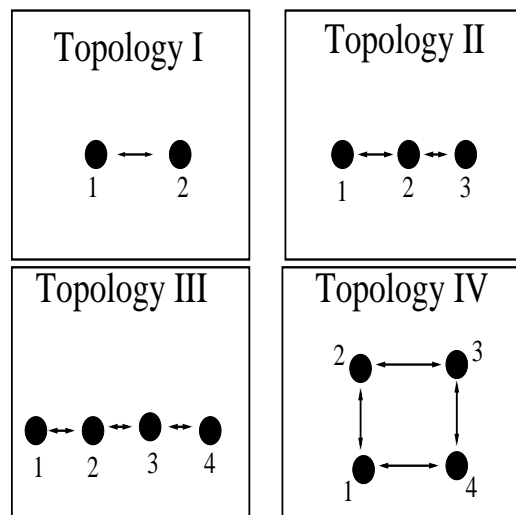


FIG. 9: Black filled circles represent a Chua's circuit and the numbers identify each circuit in the networks. Coupling is diffusible. We consider 4 topologies: 2 coupled Chua's circuit (A), an array of 3 coupled circuits, an array of 4 coupled circuits, and a ring formed by 4 coupled circuits.

considering particular values of N and t , satisfies

$$e_1 < 0.01, \quad (60)$$

then we do not change the values of N and t for the calculation of the quantities in this work. That means that if $e_1 < 0.01$, we assume that $e_1 \leq 0$. Defining a threshold or an interval to specify when a Lyapunov exponent is zero or smaller than zero is a normal procedure when calculating these exponents numerically or from experimental data. Depending on the data at hand, a numerical estimation of e_1 can provide a value arbitrarily close to zero, which would imply that our codes would be waiting an infinite amount of time until initial conditions exponentially diverge on average up to 75% of the attractor size.

So, by defining the threshold in Eq. (60), we save computational time, but T calculated from Eq. (42) will be typically underestimated (since e_1 can be much smaller) causing I_S/T to be overestimated violating inequality (3).

Our intention is to compare the exact value of the MIR between each pair of circuits, provided by I_S/T (the right-hand side of Eq. (3)) with our upper bound I_C calculated from Eq. (41) with D estimated by Eq. (43), and with our lower bound of the MIR, provided by I_C^l in Eq. (44), using \tilde{D}_0 as calculated by Eq. (30). These quantities are shown in Fig. 10(A) for connecting topology I, in Figs. 10(B) and 11 for connecting topology II, in Figs. 12,13, and 14 for connecting topology III, and in Figs. 15, 16, 17 for connecting topology IV. In each figure on the top right side (k, l) , $k, l = 1, 2, 3, 4$, indicates that we are measuring these quantities between circuits k and l . The unit of these quantities shown in these figures is $(kbits/s)$, which means that we are plotting these quantities divided by $\log(2)$.

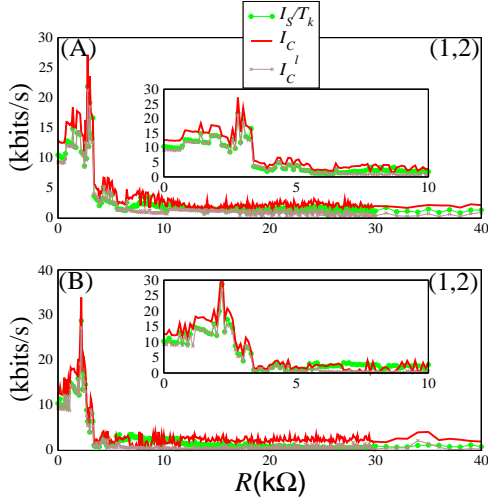


FIG. 10: [Color online] I_S/T_k as (green online) filled circles, I_C [Eq. (41)], with D estimated by Eq. (43) as the (red online) thick line, I_C^l [Eq. (44), using \tilde{D}_0 as calculated by Eq. (30)] as the (brown online) cross, for a varying coupling resistance R . (A) Topology I and (B) Topology II. The insets show a magnification of the figures for $R \in [0, 10]k\Omega$.

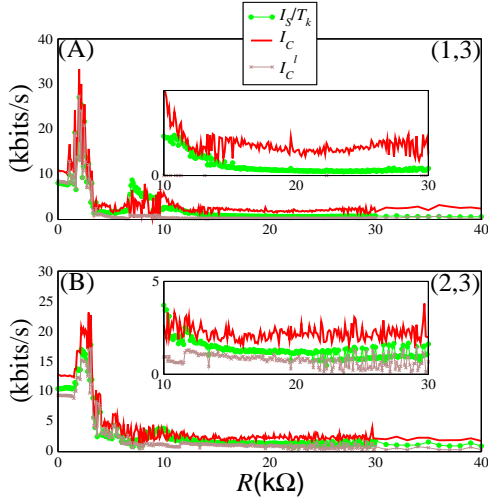


FIG. 11: [Color online] I_S/T_k as (green online) filled circles, I_C [Eq. (41)], with D estimated by Eq. (43) as the (red online) thick line, I_C^l [Eq. (44), using \tilde{D}_0 as calculated by Eq. (30)] as the (brown online) cross, for a varying coupling resistance R . We consider topology II. The insets show a magnification of the figures for $R \in [0, 10]k\Omega$.

I_S has been calculated by the method in Ref. [25]. Since we assume that the space Ω , where mutual information is being measured is 2D, we will compare our results by considering in the method of Ref. [25] a 2D space formed by the two scalar signals collected. However, we have also calculated the mutual information using in the method of Ref. [25] a 6-dimensional embedding space

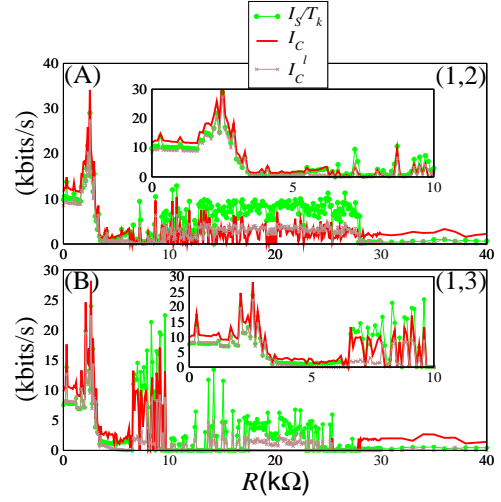


FIG. 12: [Color online] I_S/T_k as (green online) filled circles, I_C [Eq. (41)], with D estimated by Eq. (43) as the (red online) thick line, I_C^l [Eq. (44), using \tilde{D}_0 as calculated by Eq. (30)] as the (brown online) cross, for a varying coupling resistance R . We consider topology III. The insets show a magnification of the figures for $R \in [0, 10]k\Omega$.

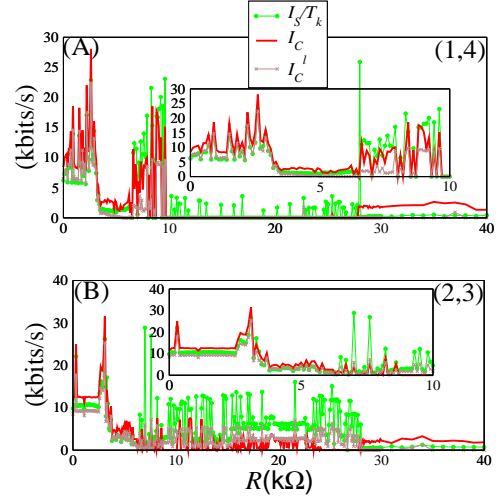


FIG. 13: [Color online] I_S/T_k as (green online) filled circles, I_C [Eq. (41)], with D estimated by Eq. (43) as the (red online) thick line, I_C^l [Eq. (44), using \tilde{D}_0 as calculated by Eq. (30)] as the (brown online) cross, for a varying coupling resistance R . We consider topology III. The insets show a magnification of the figures for $R \in [0, 10]k\Omega$.

formed by a two 3-dimensional signal obtained by reconstructing each scalar signal in a 3-dimensional embedding space. No relevant change was observed in the value for the mutual information.

In the method of Ref. [25] the phase space is partitioned in regions that contain a predefined number of points. We have obtained good results by using regions

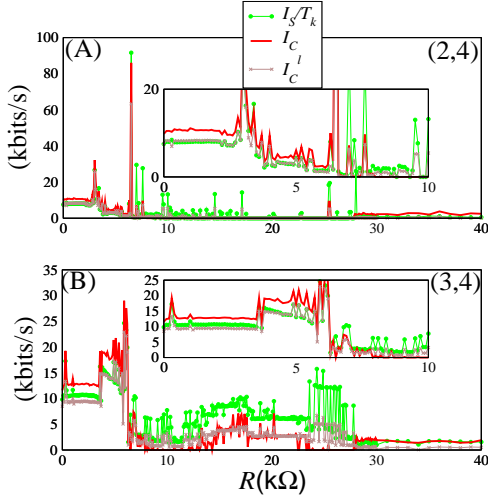


FIG. 14: [Color online] I_S/T_k as (green online) filled circles, I_C [Eq. (41)], with D estimated by Eq. (43) as the (red online) thick line, I_C^l [Eq. (44), using \tilde{D}_0 as calculated by Eq. (30)] as the (brown online) cross, for a varying coupling resistance R . We consider topology III. The insets show a magnification of the figures for $R \in [0, 10]k\Omega$.

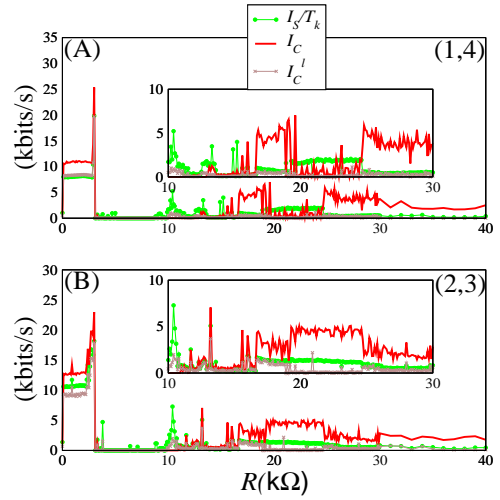


FIG. 16: [Color online] I_S/T_k as (green online) filled circles, I_C [Eq. (41)], with D estimated by Eq. (43) as the (red online) thick line, I_C^l [Eq. (44), using \tilde{D}_0 as calculated by Eq. (30)] as the (brown online) cross, for a varying coupling resistance R . We consider topology IV. The insets show a magnification of the figures for $R \in [10, 30]k\Omega$.

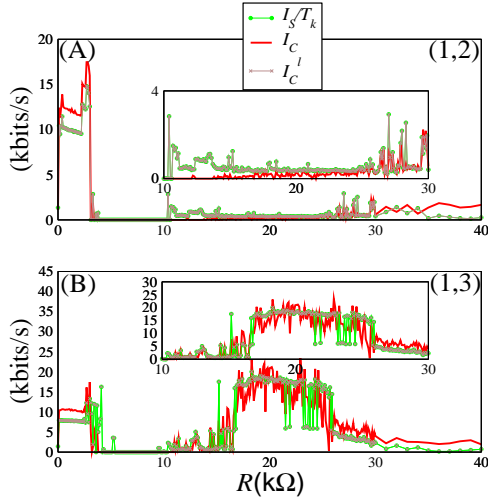


FIG. 15: [Color online] I_S/T_k as (green online) filled circles, I_C [Eq. (41)], with D estimated by Eq. (43) as the (red online) thick line, I_C^l [Eq. (44), using \tilde{D}_0 as calculated by Eq. (30)] as the (brown online) cross, for a varying coupling resistance R . We consider topology IV. The insets show a magnification of the figures for $R \in [10, 30]k\Omega$.

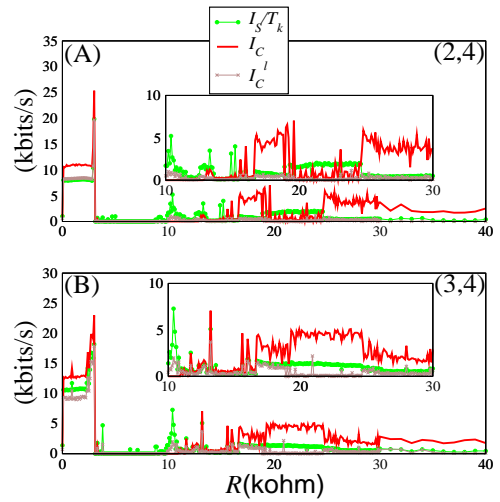


FIG. 17: [Color online] I_S/T_k as (green online) filled circles, I_C [Eq. (41)], with D estimated by Eq. (43) as the (red online) thick line, I_C^l [Eq. (44), using \tilde{D}_0 as calculated by Eq. (30)] as the (brown online) cross, for a varying coupling resistance R . We consider topology IV. The insets show a magnification of the figures for $R \in [10, 30]k\Omega$.

that contain 30 points of the continuous trajectory. By good results we mean that for large values of the resistance R , I_S/T is small, and for small values of R , I_S/T is large.

Since I_S was calculated considering regions that contain 30 points and knowing that these regions have not equal areas, to estimate T we need to imagine a box

of sides ϵ_k , such that its area ϵ_k^2 contains on average 30 points. The area occupied by the set Σ is approximately given by $\epsilon \tilde{N}_C$, where \tilde{N}_C is the number of occupied boxes. Assuming that the 79980 experimental data points occupy the attractor Σ uniformly, then on average 30 points would occupy an area of $\frac{30}{79980} \epsilon \tilde{N}_C$. The square root of this area is the side of the imaginary box that

would occupy 30 points. So, $\epsilon_k = \sqrt{\frac{30}{79980}\epsilon\tilde{N}_C}$. Then, in the following, the “exact” value of the MIR will be considered to be given by I_S/T_k , where T_k is estimated by

$$T_k = -\frac{1}{e_1} \log(\epsilon_k). \quad (61)$$

Notice that in order to estimate e_i , we use the value of t which should have the same order of magnitude of T (calculated from Eq. (42)).

B. Results and discussions

The main characteristics of the curves for the quantities I_S/T_k , I_C , and I_C^l (appearing in Figs. 10,10,11,12, 13,14,15,16, and 17) with respect to the coupling strength are:

- (a) As the coupling resistance becomes smaller, the coupling strength connecting the circuits becomes larger, the level of synchronization increases followed by an increase in I_S/T_k , I_C , and I_C^l .
- (b) All curves are near each other. As expected, for most of the resistance values, $I_C > I_S/T_k$ and $I_C^l \leq I_S/T_k$.
- (c) These networks are of the self-excitable type (see Sec. III A).
- (d) There are local minima for the MIR and the value of these minima are close to zero. These places are called “blind spots”.

The characteristic in **(a)** appears as a consequence of the fact that the larger the level of synchronization, the larger the MIR. The characteristic in **(b)** is clearly pointing that our approach provides similar result to the approach proposed in Ref. [25]. In addition, one could also calculate I_S by traditional ways and estimate the largest as well as the second largest Lyapunov exponents of the data.

The networks of Chua’s circuit studied in this work are of the type self-excitable **(c)**. A self-excitable network as defined in [14] is the one for which the MIR between nodes can be larger than the amount of information produced by a node when isolated from the network. For $R \rightarrow 0$, the circuits are almost completely synchronous. As a consequence, the values of these quantities represent approximately the amount of information produced by one Chua’s circuit if this circuit is separated from the network. For all the networks studied, we have found that I_C , I_C^l , and I_S/T_k for $R > 0$ can be larger (the maximal values of I_C , I_C^l , and I_S/T_k , for $R \in [0, 10]k\Omega$) than the values of these quantities when $R \rightarrow 0$.

For topology IV (Figs. 15,16,17), a large resistance ($R > 10k\Omega$) produces a positive and large MIR. That is a consequence of the fact that the circuits become almost

synchronous but in anti-phase. For a resistance between $5k\Omega$ and $10k\Omega$, the MIR is either zero or close to zero. Two things can contribute for producing a MIR equal or close to zero. Either one has what was called “blind” spot in Ref. [15] (characteristic **(d)**) or the network is periodic, resulting in a trajectory without positive Lyapunov exponents. The “blind spots” in **(d)** were predicted in Ref. [15] and they indicate coupling strengths for which some pair of circuits do not exchange information. A blind spot is characterized by a low value of the MIR appearing for a coupling strength such that small variations of this coupling strength makes the MIR either to be maximal or locally maximal. According to Ref. [15], a blind spot appears naturally in systems when there is as much synchronization as desynchronization between pairs of circuits. In this network a “blind” spot happens for the coupling strengths near to values that produce circuits that are synchronous but in anti-phase. These blind spots provide a clue about the connecting topology of the network [15].

For some connecting topologies and if $R > 2k\Omega$, we have obtained that $I_S/T > I_C$, which violates inequality (3). There are 2 reasons for that. The first reason is because in the calculation of T_k in Eq. (61), we have estimated the neighborhood of points ϵ_k assuming that the circuits are completely synchronous. If the circuits are not completely synchronous (what may happen when $R > 2k\Omega$) an imaginary box that would contain 30 points would have sides larger than ϵ_k . That would produce a smaller $\log(\epsilon_k)$ (since $e_k < 1$) resulting in an underestimated T_k , which would produce a larger value of the “exact” MIR, I_S/T_k , making I_S/T_k to become even larger than I_C . The second reason is because of the efforts made to save computational time (see condition (60)). Because of that, e_1 can be overestimated, resulting in an underestimated T_k and an overestimated I_S/T_k .

For a small value of the resistance, when the circuits are almost completely synchronous, the value of I_C should be close to e_1 , since $e_2 \cong 0$. In addition, as previously discussed, we expect that I_C calculated using Lyapunov exponents should be larger or equal than I_C calculated using expansion rates, since $\lambda_1 \geq e_1$. These facts can be used to test whether our results are physically consistent. The attractor of the Chua’s circuit is the Double-Scroll-like attractor. A 3D return map of the reconstructed attractor presents 4 branches, each branch with 2 minimal and 2 maximal visible points, as one can see in Fig. 18. Four minimal/maximal points renders a partition of the return map into 5 domains.

Therefore, the trajectory of this attractor can be encoded by a symbolic sequence that contains at least 20 different symbols. The average amount of information per symbol, (or per cycle of the Chua’s oscillator) contained in a symbolic sequence composed by a finite alphabet of 20 different symbols, has to be smaller or equal than $\log_2(20)$. So, the KS-entropy, H_{KS} should be smaller or equal than $\log_2(20)$. Assuming that Pesin’s equality holds (Ref. [10]), one should have that

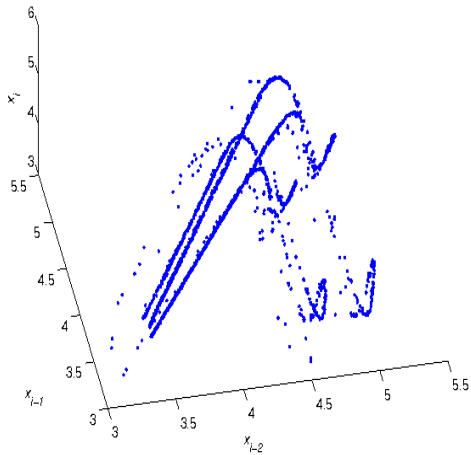


FIG. 18: Return map construct from the embedding attractor of the experimental data for 10(A) and $R = 0.1k\Omega$. From the measured variable X_i , we construct the time-delay variables that we represent by x_i : $(X(t - 2\delta t), X(t - \delta t), X(t)) = (x_{(i-2)}, x_{(i-1)}, x_{(i)})$. In order to be able to construct a Poincaré section from only one plane we take the absolute value of the time-delay variables. That simplifies analysis and visualization. If we had not taken an absolute value, the branches of the return map would be located in different regions of the space.

$\lambda_1 = H_{KS}$ and therefore, $\lambda_1 \leq \log_2(20)$ per cycle. The time the trajectory takes to make a cycle is 0.428ms, the period of a cycle. This period is the average return time of the trajectory to the Poincaré plane defined by $(x_{i-2} = 3, x_i)$. So, $\lambda_1 \leq \log_2(20)/0.4284$ bits/ms, which means that $\lambda_1 \leq 10.09$ kbits/s, a value close to I_C , $I_C^l, I_S/T_k$ for small resistance values. So, the results presented in Figs. 10,10,11,12,13,14,15,16,17 are in agreement with our previous considerations.

VII. UPPER BOUND FOR THE MIR IN DATA FROM AN EXCITABLE SYSTEM

We now simulate a system of reaction-diffusion equations that model an excitable medium, known as Barkley model [20]. In this medium, depending on the parameters considered, one sees the appearance of spiral waves.

The details about the simulations can be seen in Ref. [39]. This discrete grid is a bidimensional lattice composed of 100x100 nodes. Every node is connected to its nearest neighbors in a diffusive way. The position of a node is represented by its horizontal position in the lattice X_i , with $i \in [1, 100]$ and the vertical position in the lattice Y_j , with $j \in [1, 100]$.

We have fixed $i = 50$ and collected the time evolution of only 3000 points of the reaction kinetics variable u along the vertical nodes j . Then, we have calculated $I_C(Y_j, Y_k)$ between the signals coming from the nodes Y_j

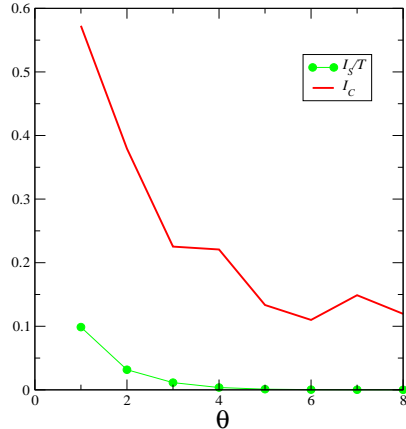


FIG. 19: I_S/T as in green filled circles and I_C as in the tick (red online) line, as a function of the distance θ between nodes X_{50}, Y_1 and X_{50}, Y_k , with $k=2, \dots, 9$

and Y_k , using Eq. (28), with $k \in [50, 59]$. The domain of the reaction kinetics variable u belongs to $[0, 1]$, so $L=\sqrt{2}$.

The Lyapunov exponents used to calculate $I_C(Y_j, Y_k)$ were obtained using the algorithm described in Ref. [40]. In order to satisfy the conditions described in Sec. VC to approximately estimate expansion rates, we consider that $q=1$ and $\epsilon = 0.05$. We set the number of minimal points in each box to be 10.

The quantity I_S is calculated using a self-contained package that does not allow us to have control of the regions of points considered to estimate mutual information. The package is based on the algorithm proposed in Ref. [41] that estimates probabilities by the distance between points in a data set. The algorithm calculates mutual information between two data sets by minimizing redundancy and maximizing relevance of patterns in the data. So, in order to compare our proposed I_C with I_S/T , being that I_S is calculated by the self-contained package that optimizes the minimal-redundancy-maximal-relevance criterion, we calculate T using the optimal value of $\epsilon = 0.05$ that permits the conditions in Sec. VC to be satisfied.

The distance between two nodes k and j is defined as $\theta = |k - j|$. We show in Fig. 19, the quantities I_S/T and I_C between the nodes Y_j and Y_k as a function of $\theta = |k - j|$, when we fix $j=50$. One can see that the larger $|k - j|$ is, the smaller $I_C(Y_{50}, Y_k)$ and $I_S/T(Y_{50}, Y_k)$ are. Very similar results are obtained if we consider different values of j , and therefore $I_C(Y_j, Y_k)$ decays as a function of the distance between the nodes (θ) in this excitable media.

VIII. I_C , AND I_C^l IN LARGER NETWORKS AND HIGHER-DIMENSIONAL SUBSPACES Ω

Imagine a network formed by K coupled oscillators. Uncoupled, each oscillator possesses a certain amount of positive Lyapunov exponents, one zero, and the others are negative. Each oscillator has dimension d . Assume that the only information available from the network are two Q dimensional measurements, or a scalar signal that is reconstructed to a Q -dimensional embedding space. So, the space Ω has dimension $2Q$, and each subspace of a node (or group of nodes) has dimension Q . To be consistent with our previous equations, we assume that we measure $M_\Omega = 2Q$ positive Lyapunov exponents on the subspace Ω . If $M_\Omega \neq 2Q$, then in the following equations $2Q$ should be replaced by M_Ω , naturally assuming that $M_\Omega \leq 2Q$.

In analogy with the derivation of Eqs. (2) and (6), we assume that if the spreading of initial conditions is uniform in the subspace Ω , then $P(i) = \frac{1}{N^Q}$ represents the probability of finding trajectory points in Q -dimensional space of one node (or a group of nodes) and $P(i, j) = \frac{1}{N^C}$ represents the probabilities of finding trajectory points in the $2Q$ -dimensional composed subspace constructed by two nodes (or two groups of nodes) in the space Ω . Additionally, we consider that the hypothetical number of occupied boxes N_C will be given by $N_C(T) = \exp^{T(\sum_{i=1}^K \lambda_i)}$. Then, if we use, for simplicity, that $L = \sqrt{2}$, we have that $T = 1/\lambda_1 \log(N)$ which lead us to

$$I_C = \lambda_1(2Q - D). \quad (62)$$

Similarly to the derivation of Eq. (6), we obtain that

$$I_C^l = \lambda_1(2Q - \tilde{D}_0). \quad (63)$$

To write Eq. (62) in terms of the positive Lyapunov exponents, we first extend Eq. (29) to larger subspaces that have dimensionality $2Q$,

$$D = 1 + \sum_{i=2}^{2Q} \frac{\lambda_i}{\lambda_1}, \quad (64)$$

where $\lambda_1 \geq \lambda_2 \geq \lambda_3 \dots \geq \lambda_{2Q}$ are the Lyapunov exponents measured on the subspace Ω . To derive this equation we only consider that the hypothetical number of occupied boxes N_C is given by $N_C(T) = \exp^{T(\sum_{i=2}^{2Q} \lambda_i)}$.

We then substitute D as a function of these exponents (Eq. (64)) in Eq. (62). We arrive that

$$I_C = (2Q - 1)\lambda_1 - \sum_{i=2}^{2Q} \lambda_i. \quad (65)$$

A. I_C as a function of the positive Lyapunov exponents of the network

Consider a network possessing M positive Lyapunov exponents, denoted by $\tilde{\lambda}_i$, $i = 1, \dots, M$. For a typical

subspace, λ_1 measured on Ω is equal to the largest Lyapunov exponent of the network. Just for the sake of simplicity in our following arguments, assume that the nodes in the network are sufficiently well connected so that in a typical measurement with a finite number of observations this property holds, i.e., $\tilde{\lambda}_1 = \lambda_1$. But, if measurements provide that $\tilde{\lambda}_1 \gg \lambda_1$, the next arguments apply as well, if one replaces λ_1 appearing in the further calculations by the smallest Lyapunov exponent, say, $\tilde{\lambda}_k$, of the network that is still larger than λ_1 , and then, substitute $\tilde{\lambda}_2$ by λ_{k+1} , and so on. As before, consider that $M_\Omega = 2Q$.

Then, for an arbitrary subspace Ω , $\sum_{i=2}^{2Q} \lambda_i \leq \sum_{i=2}^{2Q} \tilde{\lambda}_i$, since a projection cannot make the Lyapunov exponents larger, but only smaller or equal.

Defining

$$\tilde{I}_C = (2Q - 1)\lambda_1 - \sum_{i=2}^{2Q} \tilde{\lambda}_i. \quad (66)$$

Since $\sum_{i=2}^{2Q} \lambda_i \leq \sum_{i=2}^{2Q} \tilde{\lambda}_i$, it is easy to see that

$$\tilde{I}_C \leq I_C, \quad (67)$$

and therefore, I_C measured on the subspace Ω is an upper bound for \tilde{I}_C . That does not mean that more information can be obtained by the projection.

Notice that I_C depends on the projection chosen (the subspace Ω) and on its dimension, whereas \tilde{I}_C depends only on the dimension of the subspace. The same happens for the mutual information between random variables that depend on the projection considered.

Equation (66) is important because it allows us to obtain an estimation for the value of I_C analytically. As an example, imagine the following network of coupled maps with a constant Jacobian

$$X_{n+1}^{(i)} = 2X_n^{(i)} + \sigma \sum_{j=1}^K \mathbf{A}_{ij}(X_n^{(j)} - X_n^{(i)}), \text{ mod } 1, \quad (68)$$

where $X \in [0, 1]$ and \mathbf{A} represents the connecting adjacency matrix. If node j connects to node i , then $\mathbf{A}_{ij} = 1$, and 0 otherwise.

Assume that the nodes are connected all-to-all. Then, the K positive Lyapunov exponents of this network are: $\lambda_1 = \log(2)$ and $\lambda_i = \log 2[1 + \sigma]$, with $i = 2, K$. Assume also that the subspace Ω has dimension $2Q$ and that $2Q$ positive Lyapunov exponents are observed in this space and that $\lambda_1 = \lambda_1$. Substituting these Lyapunov exponents in Eq. (66), we arrive at

$$\tilde{I}_C = (2Q - 1) \log(1 + \sigma). \quad (69)$$

We conclude that there are two ways for \tilde{I}_C to become larger. Either one considers larger measurable subspaces Ω or one increases the coupling between the nodes. Then, the larger the coupling strength is, the more information is exchanged between groups of nodes.

For arbitrary topologies, one can also derive analytical formulas for \tilde{I}_C in this network, since $\tilde{\lambda}_i$ for $i > 2$ can be calculated from $\tilde{\lambda}_2$ [19]. One arrives at

$$\tilde{\lambda}_i(\omega_i\sigma/2) = \tilde{\lambda}_2(\sigma), \quad (70)$$

where ω_i is the i th largest eigenvalue (in absolute value) of the Laplacian matrix $\mathbf{L}_{ij} = \mathbf{A}_{ij} + \mathbb{I} \sum_j \mathbf{A}_{ij}$.

IX. CONCLUSIONS

This work provides lower and upper bounds for the mutual information rate (MIR) of a process whose probabilities are being generated under a dynamical rule. By a dynamical rule we mean that the spreading of nearby points can be described by either the Lyapunov exponents or the expansion rates. We have applied our theoretical findings to understand the exchange of information in systems of two linear and nonlinear coupled maps, large networks of coupled piecewise linear maps, experimental networks of Chua's circuits, and a reaction-diffusion system of equations that model an excitable media, known as Barkley model [20].

The main theoretical results of this work are:

- Two equations to calculate upper and lower bounds for the MIR exchanged between two nodes in a dynamical network as a function of Lyapunov exponents, when only a scalar signal is measured from each node, and the observational subspace Ω is bidimensional. One equation, Eq. (2), provides an upper bound as a function of the largest Lyapunov exponent and the quantity D , related to the overall spread of nearby points in the subspace Ω . This equation is appropriate to be used when the data set has few points. The other equation, Eq. (6), is a function of the largest Lyapunov exponent and of \tilde{D}_0 , the capacity dimension measured on the subspace Ω , where the MIR is being measured. This equation provides a value that is closer to the “exact” value of the MIR. However, since the capacity dimension needs to be estimated, one needs a considerably large number of points in the data set in order to be able to use it.
- Two equations to calculate upper and lower bounds for the MIR (Eqs. (41) and (44)) in terms of expansion rates. These equations extend our approach to the treatment of data sets coming from networks whose equations of motion are unknown, but that present well defined expansion rates.
- The extension of Eqs. (2) and (28) (Sec. VIII) to measure bounds for the MIR between two signals that are higher dimensional, typically signals that represent the dynamics of many nodes of a network, as a function of the Lyapunov exponents measured on a subspace defined by these nodes. We also show

how these bounds can be calculated in terms of the Lyapunov exponents of the network.

The quantity T can be thought as a “universal” time that characterizes systems possessing the deterministic character as previously defined. A small region of points is certainly mapped to a significant portion of the attractor if the system is ergodic and possesses positive Lyapunov exponents or expansion rates. And after an interval of time τ , a small initial region of points ceases spreading while being distributed over the attractor.

For the treatment of data sets, we have proposed equations for the calculations of the bounds for the MIR that depend on expansion rates. We believe that this is a natural choice if one wants to use our approach to treat data coming from complex systems. There are many reasons for this choice. Firstly, because they can be easily experimentally estimated whereas Lyapunov exponents demand huge computational efforts [26]. Secondly, because of the macroscopic nature of the expansion rates, they might be more appropriate to treat data coming from complex systems, data that have points that are not (arbitrarily) close as formally required for a proper calculation of the Lyapunov exponents. Thirdly, expansion rates can be well defined for data sets containing very few data points: the fewer points a data set contains, the larger the regions ϵ needs to be and the shorter the time T is. Finally, expansion rates are not so different from Lyapunov exponents, at least in the systems considered in this work. And since they are defined almost in the same way, some algorithms used to calculate Lyapunov exponents can be used to calculate our defined expansion rates.

The value of I_C calculated using the Lyapunov exponents is higher than if one considers expansion rates. That is a consequence of the fact that in the calculation of the Lyapunov exponents one can capture more information about the dynamics of the systems than the amount one would obtain in the calculation of expansion rates. That suggests that one can conclude that a theoretical maximal value for the MIR of a network composed by N nodes, the channel capacity of the network, is given by the maximal value of I_C , as one considers different coupling strength values and different connecting topologies.

Concerning the bounds for the MIR in higher dimensional systems, it is important to notice that we do not need to measure all the positive Lyapunov exponents of a complex network or all the expansion rates of a complex system. In Eq. (62), no matter how high is the dimension of the system, an upper bound for the MIR can be obtained if one only knows the value of the largest Lyapunov exponent (or the order-1 expansion rate) and the quantity D , related to the overall spread of nearby initial conditions on a subspace of dimension $2Q$. Alternatively, one can use Eq. (65), and then one would need to know the M_Ω largest Lyapunov exponents, being that M_Ω is a number smaller or equal than the dimension of the subspace where information is being measured, typically a

small number. In Eq. (63), a lower bound for the MIR can be calculated if one only knows the largest Lyapunov exponent and the capacity dimension of the set Σ projected on the subspace Ω of dimension $2Q$.

Acknowledgments M. S. Baptista was partially supported by the Northern Research Partnership (NRP). M. S. Baptista acknowledges the support of Alexander von

Humboldt foundation for two visits to the III. Physikalisches Institut (Univ. Göttingen) in 2010 where part of this research was conducted. M. S. Baptista would like to thank A. Politi for discussions concerning Lyapunov exponents. R.M. Rubinger, E.R. V. Junior and J.C. Sartorelli thanks the Brazilian agencies CAPES, CNPq, FAPEMIG, and FAPESP.

-
- [1] C. E. Shannon, Bell System Technical Journal **27**, 379 (1948).
- [2] L. Paninski, Neural Computation **15**, 1191 (2003).
- [3] M. Palus, V. Komárek, T. Procházka, *et al.* IEEE Engineering in Medicine and Biology **September/October**, 65 (2001).
- [4] R. Steuer, J. Kurths, C. O. Daub, J. Weise, and J. Selbig, Bioinformatics **18**, S231 (2002).
- [5] S. P. Strong, R. Koberle, R. R. de Ruyter van Steveninck, *et al.*, Phys. Rev. Lett. **80**, 197 (1998).
- [6] A. N. Kolmogorov, Dokl. Akad. Nauk SSSR **119**, 861 (1958); **124**, 754 (1959).
- [7] F. Ledrappier and J.-M. Strelcyn, Ergod. Th. & Dynam. Sys. **2**, 203 (1982).
- [8] A system that has absolutely continuous conditional measures is a system whose trajectory continuously distribute along unstable manifolds. These systems form a large class of nonuniformly hyperbolic systems [9]: the Hénon family; Hénon-like attractor arising from Homoclinic bifurcations; strange attractors arising from Hopf Bifurcations (e.g. Rössler oscillator); some classes of mechanical models with periodic forcing. The result in Ref. [7] extends a previous result by Pesin [10] that demonstrated that for hyperbolic maps, the KS entropy is equal to the sum of the positive Lyapunov exponents.
- [9] L.-S. Young, Journal of Statistical Physics **108**, 733, (2002).
- [10] Ya. B. Pesin, Russ. Math. Surv. **32**, 55 (1977).
- [11] D. Ruelle, Bol. Soc. Bras. Mat. **9**, 83 (1978).
- [12] J.F. Donges, Y. Zou, N. Marwan, and J. Kurths, Eur. Phys. J. **174**, 157 (2009).
- [13] M. S. Baptista and J. Kurths, Phys. Rev. E **72**, 045202(R) (2005).
- [14] M. S. Baptista and J. Kurths, Phys. Rev. E **77**, 026205 (2008).
- [15] M. S. Baptista, J. X. de Carvalho, M. S. Hussein, PloS ONE **3**, e3479 (2008). See also <http://arxiv.org/abs/0804.298>.
- [16] The BCLEs are the Lyapunov exponents along a trajectory on the synchronisation manifold. Even when the nodes of a network have an asymptotic solution, which is far away from the synchronization manifold, the BCLEs can be calculated, since in their calculation we use a trajectory that lies on the synchronisation manifold. The BCLEs describe the exponential divergence of nearby trajectories along the synchronization manifold and along all the directions transversal to the synchronization manifold.
- [17] L. M. Pecora and T. L. Carrol, Phys. Rev. A **44**, 2374 (1991).
- [18] Like the BCLEs, the conditional Lyapunov exponents (CLEs) are calculated using the variational equation of the network linearly expanded around the synchronous solution. This variational equation is a function of a synchronous trajectory. However, as it was originally defined [17], for the calculation of the CLEs one inputs in the variational equation the trajectory of one node of the network, which might not be synchronous. When the trajectory of this reference node is close to the synchronization manifold, then the CLEs become close to the BCLEs.
- [19] M. S. Baptista, F. M. Kakmeni, G. L. Magno, M. S. Hussein, Phys. Lett. A **375**, 1309 (2011).
- [20] D. Barkley D, M. Kness, and L. S. Tuckerman, Phys. Rev. A **42** (1990).
- [21] J. D. Farmer, E. Ott, and J. A. Yorke, Physica D **7**, 153 (1983).
- [22] M. S. Baptista, D. M. Maranhão, J. C. Sartorelli, Chaos, **19**, 043115 (2009).
- [23] P. R. F. Pinto, M. S. Baptista, I. Labouriau, Communications in Nonlinear Science and Numerical Simulation **16**, 863 (2011).
- [24] J. B. Gao, Phys. Rev. Lett. **83**, 3178 (1999).
- [25] A. Kraskov, H. Stogbauer, and P. Grassberger, Phys. Rev. E **68**, 066138 (2004).
- [26] P. So, E. Barreto, B. R. Hunt, Phys. Rev. E **60**, 378 (1999).
- [27] P. Grassberger, R. Badii, and A. Politi, J. Stat. Phys. **51**, (1988).
- [28] A. Prasad and R. Ramaswamy, Phys. Rev. E **60**, 2761, (1999).
- [29] R. Badii and A. Politi, Phys. Rev. A **35**, 1288 (1987).
- [30] E. Ott, T. Sauer, and J. A. Yorke, Phys. Rev. A **39**, 4212 (1989).
- [31] W. Jezewski, Physics Letters A **183**, 63 (1993).
- [32] J. Schreiber, Discrete and Continuous Dynamical Systems **3**, 433 (1997).
- [33] E. Aurell, G. Boffetta, A. Crisanti, *et al.*, Phys. Rev. Lett. **77**, 1262 (1966).
- [34] H. Kantz, Phys. Lett. A **185**, 77 (1994).
- [35] M. T. Rosenstein, J. J. Collins, C. J. De Luca, Physica D **65**, 117 (1993).
- [36] D. Ruelle and F. Takens, Commun. Math. Phys. **20**, 167 (1971).
- [37] T. Matsumoto, Proc. IEEE **75**, 1033 (1987).
- [38] H. A. Albuquerque, R. M. Rubinger, P. C. Rech, Physics D **233**, 66 (2007).
- [39] P. Bittihn, G. Luther, E. Bodenschatz, *et al.*, New Journal of Physics **10**, 103012 (2008).
- [40] T. Pereira, *et al.*, Phys. Rev. E **73**, 017201 (2006).
- [41] H. Peng, F. Long, and C. Ding, IEEE Transactions on pattern analysis and machine intelligence **27**, 1226 (2005).